Lightness of Higgs boson and spontaneous *CP* violation in the Lee model

Ying-nan Mao[1] and Shou-hua Zhu[1,2,3]

[1]*Institute of Theoretical Physics and State Key Laboratory of Nuclear Physics and Technology, Peking University, Beijing 100871, China*

[2]*Collaborative Innovation Center of Quantum Matter, Beijing 100871, China*

[3]*Center for High Energy Physics, Peking University, Beijing 100871, China*

(Received 2 October 2014; published 30 December 2014)

We proposed a mechanism in which the lightness of Higgs boson and the smallness of charge parity (*CP*) violation are correlated based on the Lee model, namely, the spontaneous *CP*-violation two-Higgs-doublet model. In this model, the mass of the lightest Higgs boson m_h as well as the quantities K and J are $\propto t_\beta s_\xi$ in the limit $t_\beta s_\xi \to 0$ (see text for definitions of t_β and ξ), namely, the *CP* conservation limit. Here, K and J are the measures for *CP*-violation effects in scalar and Yukawa sectors, respectively. It is a new way to understand why the Higgs boson discovered at the LHC is light. We investigated the important constraints from both high energy LHC data and numerous low energy experiments, especially the measurements of electric dipole moments of electron and neutron as well as the quantities of B meson and kaon. Confronting all data, we found that this model is still viable. It should be emphasized that there is no standard-model limit for this scenario; thus it is always testable for future experiments. In order to pin down the Lee model, it is important to discover the extra neutral and charged Higgs bosons and measure their *CP* properties and the flavor-changing decays. At the LHC with $\sqrt{s} = 14$ TeV, this scenario is favored if there is significant suppression in the $b\bar{b}$ decay channel or any vector boson fusion, V + H production channels. On the contrary, it will be disfavored if the signal strengths are standard-model–like more and more. It can be easily excluded at $(3\text{–}5)\sigma$ level with several fb^{-1} at future e^+e^- colliders, via accurately measuring the Higgs boson production cross sections.

DOI: 10.1103/PhysRevD.90.115024 PACS numbers: 12.60.Cn, 12.60.Fr

I. INTRODUCTION

How to realize the electroweak gauge symmetry breaking and charge parity (*CP*) violation is an important topic in the standard model (SM) and beyond the SM (BSM) in particle physics. In order to induce the spontaneous gauge symmetry breaking, the Higgs mechanism was proposed in 1964 [1]. Meanwhile, in the SM the *CP* violation was put by hand via the complex Yukawa couplings among Higgs field and fermions, namely, the Kobayashi and Maskawa (KM) mechanism [2]. In 1973, Kobayashi and Maskawa [2] proposed that if there are three generations of fermions, there would be a nontrivial phase that leads to *CP* violation in the fermion mixing matrix (CKM matrix [2,3]). In a word, one single scalar field plays the two-fold roles. In the SM, only one doublet Higgs field is introduced. After spontaneous symmetry breaking, there exists one physical scalar, the Higgs boson. It is essential to discover and measure the properties of the Higgs boson, in order to test the SM or discover the BSM.

A. Status of experimental measurements on new scalar boson

Experimentally, in July, 2012, both CMS [4] and ATLAS [5] discovered a new boson with the mass around 125.7 GeV in $\gamma\gamma$ and ZZ^* final states with the luminosity of about 10 fb^{-1}. At the LHC, the SM Higgs boson can be produced through the following three processes: (1) gluon-gluon fusion (ggF); (2) vector boson fusion (VBF); and (3) associated production with a vector boson (V + H). It can also be produced associated with a pair of top quarks due to the large m_t, but the cross section is suppressed by its phase space and parton distribution function (PDF) of protons. A SM Higgs boson would mainly decay to fermion pairs ($b\bar{b}, \tau^+\tau^-$, or $t\bar{t}$ if heavier than $2m_t$), massive gauge boson pair (W^+W^-, Z^0Z^0), massless gauge boson pair ($gg, \gamma\gamma$), etc. The decay properties for a 125.7 GeV SM Higgs boson are listed in Table I; for the production and decay properties, see also the reviews [6] and [7].

The updated searches by CMS [8–11] and ATLAS [12–15] with the luminosity of about 25 fb^{-1} till the end of 2012[1] gave the significance s and signal strengths μ (defined as the ratios between observed $\sigma \cdot \mathrm{Br}$ and the corresponding SM prediction) for some channels. Because the measurements will be utilized to constrain the new model in this paper, we list the results in Table II for CMS and Table III for ATLAS.[2] The new boson has a combined mass 125.7 GeV and it is also favored as a 0^+ particle in

[1]Some new analyses updated in 2014 are used as well, which modify the old results a little bit.

[2]The VBF events are usually easy to tag with two jets that have large invariant mass, while sometimes it is difficult to tag a gluon fusion event.

TABLE I. Table for the SM prediction for the decay branching ratios of a 125.7 GeV Higgs boson; the numbers are from [7].

Decay channel	Branching ratio (%)	Relative uncertainty (%)
$b\bar{b}$	56.6	± 3.3
$c\bar{c}$	2.85	± 12.2
$\tau^+\tau^-$	6.21	± 5.6
gg	8.51	$^{+10.2}_{-9.9}$
WW^*	22.6	$^{+4.2}_{-4.1}$
ZZ^*	2.81	$^{+4.2}_{-4.1}$
$\gamma\gamma$	0.228	± 4.9
$Z\gamma$	0.16	$^{+8.9}_{-8.8}$
Total width	4.17 MeV	± 3.9

TABLE II. Signal strengths for some production and decay channels of the new boson at CMS (with combined significance over 3σ).

	μ(VBF/V + H)	μ(ggF)	μ(combined)	Significance
$\gamma\gamma$	$1.58^{+0.77}_{-0.68}$	$1.12^{+0.37}_{-0.32}$	$1.14^{+0.26}_{-0.23}$	5.7σ
ZZ^*	$1.7^{+2.2}_{-2.1}$	$0.80^{+0.46}_{-0.36}$	$0.93^{+0.29}_{-0.25}$	6.8σ
WW^*	$0.60^{+0.57}_{-0.46}$	$0.74^{+0.22}_{-0.20}$	$0.72^{+0.20}_{-0.18}$	4.3σ
$\tau^+\tau^-$	0.94 ± 0.41		0.78 ± 0.27	3.2σ

TABLE III. Signal strengths for some production and decay channels of the new boson at ATLAS (with combined significance over 3σ).

	μ(VBF/V + H)	μ(ggF)	μ(combined)	Significance
$\gamma\gamma$	0.8 ± 0.7	1.32 ± 0.38	1.17 ± 0.27	5.2σ
ZZ^*	$0.26^{+1.64}_{-0.94}$	$1.66^{+0.51}_{-0.44}$	$1.43^{+0.40}_{-0.33}$	8.1σ
WW^*	$1.28^{+0.53}_{-0.45}$	$1.01^{+0.28}_{-0.26}$	$1.09^{+0.23}_{-0.20}$	6.1σ
$\tau^+\tau^-$	$1.24^{+0.58}_{-0.54}$	$1.93^{+1.45}_{-1.15}$	$1.42^{+0.44}_{-0.38}$	4.5σ

spin and parity by the data [9,16,17] if we assume that there is no CP violation induced by this boson.

The experimental measurements of the new particle are in agreement with the SM predictions within the current accuracy. In the SM the electroweak fitting results [18] also favor a light one. It allows a SM Higgs boson lighter than 145 GeV at 95% C.L. inferred from the oblique parameters [19] with fixed $U = 0$. However, there is still spacious room for the BSM. For example, if we assume that the new particle is a CP-mixing state, the general effective interaction for hZZ can be written as [9,20,21]

$$\mathcal{L}_{hZZ} = \frac{h}{v}\left(a_1 m_Z^2 Z^\mu Z_\mu + \frac{1}{2}a_2 Z_{\mu\nu}Z^{\mu\nu} + \frac{1}{2}a_3 Z_{\mu\nu}\tilde{Z}^{\mu\nu}\right) \quad (1)$$

with $\tilde{Z}_{\mu\nu} = (1/2)\epsilon_{\mu\nu\alpha\beta}Z^{\alpha\beta}$. Define

$$f_{a3} = \frac{(a_3/a_1)^2}{(a_3/a_1)^2 + \sigma_1/\sigma_3} \quad (2)$$

where $\sigma_{1(3)}$ is the partial width for a pure CP even (odd) state with $a_{1(3)} = 1$. Direct search by CMS gives $f_{a3} < 0.47$ at 95% C.L., which leads to $|a_3/a_1| < 2.4$ [9]. In a renormalized theory, a_2 and a_3, which are loop induced, are expected to behave as $a_{2,3}/a_1 \ll \mathcal{O}(1)$, so they are still not constrained by current LHC data.

B. The issue of lightness of new scalar boson in the SM and BSM

BSM is well motivated because the SM cannot account for the matter-dominant Universe and provide the suitable dark matter candidate. However, BSM scale is usually pushed to a much higher value than that of weak interaction, given the great success of the SM. In such circumstance, the 125.7 GeV scalar boson is unnatural. In other words, the lightness of the new scalar must link to a certain mechanism. The issue of the lightness of the new scalar differs in the SM and BSM. In the SM, we cannot predict the mass of Higgs boson, and the Higgs boson with the mass 125.7 GeV simply implies that the interactions are in the weak regime. For example, the Higgs boson self-coupling

$$\lambda = \frac{m_h^2}{2v^2} = 0.13 \ll 1. \quad (3)$$

Compared with the strong interactions at low energy, the mass of σ particle [or we call it $f_0(600)$, which plays a similar role as the Higgs boson) $m_\sigma \gg f_\pi (\approx 93$ MeV) appears at a typical scale $\Lambda \sim 4\pi f_\pi \sim \mathcal{O}(1)$ GeV. Thus, we can argue that the new boson with mass 125.7 GeV is rather light compared with the strong interaction. As a side remark, the pion mass $m_\pi \sim \mathcal{O}(f_\pi)$ is light compared with σ due to the approximate chiral symmetry. This has motivated the idea that the new scalar boson may be the pseudo–Nambu-Goldstone boson for certain unknown symmetry breaking.

Theoretically, in some BSM models there exists a light scalar naturally. For example, (1) in the minimal supersymmetric model, the lightest Higgs boson should be lighter than 140 GeV including higher-order corrections [22] (at tree level it should be lighter than the mass of Z_0 boson); (2) in the little Higgs model, a Higgs boson that is treated as a pseudo–Nambu-Goldstone boson must be light due to classical global symmetry and it acquires mass through quantum effects only [23]; (3) similarly, anomalies in scale invariance can also generate a light Higgs boson as well [24]; and (4) the lightness of Higgs boson can intimately connect with the spontaneous CP violation [25]. While the first three approaches are based on the conjectured symmetry, the last one utilizes the observed approximate CP symmetry. Historically, Lee proposed the

spontaneous *CP* violation in 1973 [26] as an alternative way to induce *CP* violation. For the fourth approach, Lee's idea is extended to account for the lightness of the observed Higgs boson.

C. The lightness of new scalar boson and spontaneous *CP* violation

CP violation was first discovered in neutral K meson in 1964 [27]. Experimentally, people have already measured several kinds of *CP*-violated effects in neutral K and B meson, and charged B-meson systems [28]. This *CP* violation can be successfully accounted for by the CKM matrix, which is usually parametrized as the Wolfenstein formalism [29]

$$V_{\rm CKM} = \begin{pmatrix} 1-\lambda^2/2 & \lambda & A\lambda^3(\rho-i\eta) \\ -\lambda & 1-\lambda^2/2 & A\lambda^2 \\ A\lambda^3(1-\rho-i\eta) & -A\lambda^2 & 1 \end{pmatrix} + \mathcal{O}(\lambda^4). \tag{4}$$

The Jarlskog invariant [28,30]

$$J = A^2\lambda^6\eta = (3.06^{+0.21}_{-0.20}) \times 10^{-5} \tag{5}$$

measures the *CP* violation in flavor sector. The smallness of J means the smallness of *CP* violation in the real world in the SM. Another possible explicit *CP* violation comes from the θ term

$$\mathcal{L}_{\rm str} = \frac{\theta\alpha_s}{8\pi} G_{\mu\nu}\tilde{G}^{\mu\nu} \tag{6}$$

in the QCD Lagrangian [31,32]. The parameter θ is strongly constrained by the neutron electric dipole moment (EDM) measurement [33,34], namely, $|\theta| \lesssim 10^{-10}$. Why θ is extremely small is known as the strong *CP* problem. It is often interesting, necessary, and useful to search for other sources of *CP* violation beyond the KM mechanism. As a common reason, for example, *CP* violation is one of the conditions needed to produce the matter-antimatter asymmetry in the Universe today [35], but the SM itself cannot provide the first order electroweak phase transition and large enough *CP* violation to get the right asymmetry between matter and antimatter [28,36–38].

In 1973, Lee proposed a two-Higgs-doublet model (2HDM; Lee model) [26] in which all parameters in the scalar potential are real but it is possible to leave a nontrivial phase ξ between the vacuum expectation values (VEV) of the two Higgs doublets. *CP* can be spontaneously broken in this model. Chen *et al.* [39] proposed the possibility that the complex vacuum could lead to a correct CKM matrix, which means that we can set all Yukawa couplings to be real; thus, the complex vacuum would become the only source of *CP* violation. It is also a possible way to solve strong *CP* problem, for example, in spontaneous *CP*-violation scenarios, θ arises only from the determinant of quark mass matrix. Assuming $\theta \equiv 0$ at tree level, the loop corrections can generate naturally small θ [40,41], the so-called "calculable θ" [31]. Without imposing symmetry [42], the Yukawa couplings are arbitrary, which will generate the flavor-changing neutral currents (FCNC) at tree level. FCNC are severely constrained by experiments. Cheng and Sher proposed an ansatz [43] that the flavor-changing couplings should be $\propto \sqrt{m_i m_j}$ for two fermions with mass m_i and m_j. One of the authors of this paper had proposed a mechanism [25] to understand the lightness of Higgs boson in the $\xi \to 0$ limit. In this paper, we will explore the relation between the smallness of *CP* violation and the lightness of Higgs boson in a similar way as the Lee model further. Specifically, we will study the full phenomenology of the Lee model to see whether this model is still viable to confront LHC data and numerous low energy measurements.

We should mention that there are also cosmological implications for the Lee model. In this model, *CP* is a spontaneously broken discrete symmetry; thus, it may face the domain wall problem [44] during the electroweak phase transition. It is argued that if there is a small initial bias, and thus one of the vacuum states is favored, the domain walls would disappear soon [44,45], for example, if there is small explicit *CP* violation [46]. In the soft *CP* breaking model, the electroweak baryogenesis effects are estimated by Cohen *et al.* [38] at early time, and was estimated again by Shu and Zhang [47] after including LHC data. They found that the observed matter-antimatter asymmetry can be explained. It is also discussed numerically that an inflation during the symmetry breaking would forbid the domain wall production [48].

This paper is organized as follows. Section II presents the Lee model and the scenario that lightness of Higgs boson and smallness of *CP* violation are correlated. Sections III–IV contain the constraints on the Lee model from high energy and low energy data, respectively. Section V studies the perspectives for the Lee model for future experiments. The last section collects our conclusions and discussions.

II. THE LEE MODEL: MASS SPECTRUM AND COUPLINGS

We begin with the description of the Lee model [26] assuming that in the whole Lagrangian there are no explicit *CP*-violation terms, which means all the *CP*-violation effects come from a complex vacuum.[3] For the Lee model, the interactions of scalar fields read [26]

[3]For a review on 2HDM, the interested reader can read Ref. [49].

$$\mathcal{L} = (D_\mu \phi_1)(D^\mu \phi_1) + (D_\mu \phi_2)(D^\mu \phi_2) - V(\phi_1, \phi_2). \quad (7)$$

Here,

$$\phi_1 = \begin{pmatrix} \phi_1^+ \\ \frac{v_1 + R_1 + iI_1}{\sqrt{2}} \end{pmatrix}, \qquad \phi_2 = \begin{pmatrix} \phi_2^+ \\ \frac{v_2 e^{i\xi} + R_2 + iI_2}{\sqrt{2}} \end{pmatrix} \quad (8)$$

are the two Higgs doublets. We can get the masses of gauge bosons

$$m_W = \frac{g\sqrt{v_1^2 + v_2^2}}{2}, \qquad m_Z = \frac{\sqrt{(g^2 + g'^2)(v_1^2 + v_2^2)}}{2} \quad (9)$$

by setting $v = \sqrt{v_1^2 + v_2^2} = 246$ GeV. Defining $R(I)_{ij}$ as the real (imaginary) part of $\phi_i^\dagger \phi_j$, we can write a general potential as

$$\begin{aligned} V &= V_2 + V_4 \\ &= \mu_1^2 R_{11} + \mu_2^2 R_{22} + \lambda_1 R_{11}^2 + \lambda_2 R_{11} R_{12} + \lambda_3 R_{11} R_{22} \\ &\quad + \lambda_4 R_{12}^2 + \lambda_5 R_{12} R_{22} + \lambda_6 R_{22}^2 + \lambda_7 I_{12}^2, \end{aligned} \quad (10)$$

in which we can always perform a rotation between ϕ_1 and ϕ_2 to keep the coefficient of R_{12} term zero in V_2. We can also write the general Yukawa couplings as

$$\begin{aligned} \mathcal{L}_y = &-\bar{Q}_{Li}(Y_{1d}\phi_1 + Y_{2d}\phi_2)_{ij} D_{Rj} \\ &- \bar{Q}_{Li}(Y_{1u}\tilde{\phi}_1 + Y_{2u}\tilde{\phi}_2)_{ij} U_{Rj}, \end{aligned} \quad (11)$$

in which $\tilde{\phi}_i = i\sigma_2 \phi_i^*$ and all Yukawa couplings are real.

By minimizing the Higgs potential, and for some parameter choices, we can get a nonzero phase difference ξ between two Higgs VEVs, which would induce spontaneous CP violation. We can always perform a gauge transformation to get at least one of the VEVs real like in (8). When $v_1, v_2, \xi \neq 0$, we can express

$$\mu_1^2 = -\lambda_1 v_1^2 - \frac{\lambda_3 + \lambda_7}{2} v_2^2 - \frac{\lambda_2}{2} v_1 v_2 \cos\xi; \quad (12)$$

$$\mu_2^2 = -\frac{\lambda_3 + \lambda_7}{2} v_1^2 - \lambda_6 v_2^2 - \frac{\lambda_5}{2} v_1 v_2 \cos\xi. \quad (13)$$

$\tan\beta$ is identified as v_2/v_1 as usual. We also have an equation about ξ,

$$\frac{\lambda_2}{2} v_1^2 + \frac{\lambda_5}{2} v_2^2 + (\lambda_4 - \lambda_7) v_1 v_2 \cos\xi = 0, \quad (14)$$

which requires $\lambda_2 v_1^2 + \lambda_5 v_2^2 < 2|\lambda_4 - \lambda_7| v_1 v_2$. Of course, the couplings λ_i must keep the vacuum stable; for the conditions see Sec. A for details.

All the CP-violation effects in the real world are small (see the data in [28]), corresponding to the smallness of the off-diagonal elements in the CKM matrix that leads to the smallness of the Jarlskog invariant. As a limit, when $t_\beta \equiv \tan\beta \to 0$,[4] or we may write $t_\beta s_\xi \to 0$ instead since $|s_\xi| < 1$ always holds, there would be no CP violation in the scalar sector. The CKM matrix would be real; thus, there would be no CP violation in the flavor sector as well. In this paper we will consider the small t_β limit, in which all CP-violation effects tend to zero as $t_\beta \to 0$. We treat the whole world as an expansion around the point without CP violation.

The two Higgs doublets contain eight degrees of freedom, three of which should be eaten by massive gauge bosons as Goldstones. So there are five physical scalars left, two of which are charged and three of which are neutral. If CP is a good symmetry, there will be two CP even and one CP odd scalar among the three neutral ones. However, when CP is spontaneously breaking, the CP eigenstates will mix with each other; thus, the neutral scalars have no certain CP charge. We have the Goldstones as

$$G^\pm = c_\beta \phi_1^\pm + e^{\mp i\xi} \phi_2^\pm; \quad (15)$$

$$G^0 = c_\beta I_1 + s_\beta c_\xi I_2 - s_\beta s_\xi R_2. \quad (16)$$

The charged Higgs boson is the orthogonal state of the charged Goldstone as

$$H^\pm = -e^{\pm i\xi} s_\beta \phi_1^\pm + c_\beta \phi_2^\pm \quad (17)$$

and its mass square should be

$$m_{H^\pm}^2 = -\frac{\lambda_7 v^2}{2}, \quad (18)$$

while for the neutral part, we write the mass square matrix as $\tilde{m} v^2/2$ in the basis $(-s_\beta I_1 + c_\beta c_\xi I_2 - c_\beta s_\xi R_2, R_1, s_\xi I_2 + c_\xi R_2)^T$. The symmetric matrix $\tilde{m}$ is

[4]We write $s_\alpha \equiv \sin\alpha$, $c_\alpha \equiv \cos\alpha$, $t_\alpha \equiv \tan\alpha$ for short in this paper.

$$\begin{pmatrix} (\lambda_4-\lambda_7)s_\xi^2 & -((\lambda_4-\lambda_7)s_\beta c_\xi & -((\lambda_4-\lambda_7)c_\beta c_\xi \\ & +\lambda_2 c_\beta)s_\xi & +\lambda_5 s_\beta)s_\xi \\ & 4\lambda_1 c_\beta^2 + 2\lambda_2 c_\beta s_\beta c_\xi & (2(\lambda_3+\lambda_7)+(\lambda_4-\lambda_7)c_\xi^2)s_\beta c_\beta \\ & +(\lambda_4-\lambda_7)s_\beta^2 c_\xi^2 & +\lambda_2 c_\beta^2 c_\xi + \lambda_5 s_\beta^2 c_\xi \\ & & (\lambda_4-\lambda_7)c_\beta^2 c_\xi^2 \\ & & +2\lambda_5 s_\beta c_\beta c_\xi + 4\lambda_6 s_\beta^2 \end{pmatrix}, \tag{19}$$

and its three eigenvalues correspond to the masses of three neutral bosons.

We expand the matrix $\tilde{m}$ in series of $t_\beta(s_\xi)$ as

$$\tilde{m} = \tilde{m}_0 + (t_\beta s_\xi)\tilde{m}_1 + (t_\beta s_\xi)^2\tilde{m}_2 + \cdots \tag{20}$$

to get the approximate analytical behavior of its eigenvalues and eigenstates. Certainly, we have

$$\lim_{t_\beta s_\xi \to 0} \det(\tilde{m}) = \det(\tilde{m}_0) = 0, \tag{21}$$

which means a zero eigenvalue of $\tilde{m}_0$; thus, there must be a light neutral scalar when $t_\beta s_\xi$ is small. To the leading order of $t_\beta s_\xi$, for the lightest scalar h, we have

$$\begin{aligned} m_h^2 &= \frac{v^2 t_\beta^2 s_\xi^2}{2}\left(\frac{(\tilde{m}_1)_{12}^2}{(\tilde{m}_0)_{22}} + \frac{(\tilde{m}_1)_{13}^2}{(\tilde{m}_0)_{33}} + (\tilde{m}_2)_{11}\right) \\ &= \frac{v^2 t_\beta^2 s_\xi^2}{2}\left[4(\lambda_3+\lambda_7)^2\left(\frac{c_\theta^2}{(\tilde{m}_0)_{22}} + \frac{s_\theta^2}{(\tilde{m}_0)_{33}}\right) + \lambda_5^2\left(\frac{s_\theta^2}{(\tilde{m}_0)_{22}} + \frac{c_\theta^2}{(\tilde{m}_0)_{33}}\right) - 2\lambda_5(\lambda_3+\lambda_7)s_{2\theta}\left(\frac{1}{(\tilde{m}_0)_{22}} - \frac{1}{(\tilde{m}_0)_{33}}\right) + 4\lambda_6\right]; \end{aligned} \tag{22}$$

$$\begin{aligned} h &= I_2 + t_\beta s_\xi\left(\frac{(\tilde{m}_1)_{12}}{(\tilde{m}_0)_{22}}(c_\theta R_1 + s_\theta R_2) + \frac{(\tilde{m}_1)_{13}}{(\tilde{m}_0)_{33}}(c_\theta R_2 - s_\theta R_1) - \frac{I_1}{t_\xi}\right) \\ &= I_2 + t_\beta s_\xi\left[\left(2(\lambda_3+\lambda_7)\left(\frac{c_\theta^2}{(\tilde{m}_0)_{22}} + \frac{s_\theta^2}{(\tilde{m}_0)_{33}}\right) + \frac{\lambda_5 s_{2\theta}}{2}\left(\frac{1}{(\tilde{m}_0)_{22}} - \frac{1}{(\tilde{m}_0)_{33}}\right)\right)R_1 + \left((\lambda_3+\lambda_7)s_{2\theta}\left(\frac{1}{(\tilde{m}_0)_{22}} - \frac{1}{(\tilde{m}_0)_{33}}\right)\right. \right. \\ &\quad \left.\left. + \lambda_5\left(\frac{s_\theta^2}{(\tilde{m}_0)_{22}} + \frac{c_\theta^2}{(\tilde{m}_0)_{33}}\right)\right)R_2 - \frac{I_1}{t_\xi}\right], \end{aligned} \tag{23}$$

while for the two heavier neutral Higgs bosons, we have

$$m_{2(3)}^2 = \frac{v^2}{2}((\tilde{m}_0)_{22(33)} + \mathcal{O}(t_\beta s_\xi)), \tag{24}$$

in which $(\tilde{m}_0)_{22(33)}$ are the other two eigenvalues of $\tilde{m}_0$ and

$$\begin{aligned} (\tilde{m}_0)_{22(33)} &= \frac{4\lambda_1 + \lambda_4 - \lambda_7}{2} \\ &\quad \pm \left(\frac{4\lambda_1 - (\lambda_4 - \lambda_7)}{2}c_{2\theta} + \lambda_2 s_{2\theta}\right), \end{aligned} \tag{25}$$

where $\theta = (1/2)\arctan(2\lambda_2/(4\lambda_1 - \lambda_4 + \lambda_7))$. The physical states are

$$\begin{pmatrix} h_2 \\ h_3 \end{pmatrix} = \begin{pmatrix} c_\theta & s_\theta \\ -s_\theta & c_\theta \end{pmatrix}\begin{pmatrix} R_1 \\ R_2 \end{pmatrix} + \mathcal{O}(t_\beta s_\xi). \tag{26}$$

For all the details about scalar spectra and their small $t_\beta s_\xi$ expansion series, the interested reader can see Sec. B.

From the Yukawa couplings we will get the mass matrices for fermions as

$$(M_U)_{ij} = \frac{v}{\sqrt{2}}(Y_{1u}c_\beta + Y_{2u}s_\beta e^{-i\xi})_{ij}, \tag{27}$$

$$(M_D)_{ij} = \frac{v}{\sqrt{2}}(Y_{1d}c_\beta + Y_{2d}s_\beta e^{i\xi})_{ij}. \tag{28}$$

We can always perform the diagonalization for $M_{U(D)}$ with matrices $U(D)_L$ and $U(D)_R$ as

$$U_L M_U U_R^\dagger = \begin{pmatrix} m_u & & \\ & m_c & \\ & & m_t \end{pmatrix},$$
$$D_L M_D D_R^\dagger = \begin{pmatrix} m_d & & \\ & m_s & \\ & & m_b \end{pmatrix}. \quad (29)$$

And $V_{\rm CKM} = U_L D_L^\dagger$ is the CKM matrix.

In this scenario, the couplings for the discovered light Higgs boson should be modified from the SM by a factor as

$$\mathcal{L}_{h,\rm eff} = c_V\left(\frac{2m_W^2}{v}W_\mu^+ W^{\mu-} + \frac{m_Z^2}{v}Z_\mu Z^\mu\right)h - c_\pm v H^+ H^- h - \sum_i (c_{Ui}\bar{U}_{Li}U_{Ri} + c_{Di}\bar{D}_{Li}D_{Ri} + \text{H.c.})h, \quad (30)$$

where the factors $c_\pm$ and c_V must be real, but c_{Ui} and c_{Di} may be complex. According to (C1)–(C4) in Sec. C, to the leading order of $t_\beta s_\xi$, we straightforwardly have

$$c_V = t_\beta s_\xi(1+\eta_1); \quad (31)$$

$$c_{Di} = \frac{t_\beta s_\xi}{\sqrt{2}}(\eta_1(Y'_{1d})_{ii} + \eta_2(Y'_{2d})_{ii}) + \frac{i(Y'_{2d})_{ii}}{\sqrt{2}}; \quad (32)$$

$$c_{Ui} = \frac{t_\beta s_\xi}{\sqrt{2}}(\eta_1(Y'_{1u})_{ii} + \eta_2(Y'_{2u})_{ii}) - \frac{i(Y'_{2u})_{ii}}{\sqrt{2}}; \quad (33)$$

and the coupling including charged Higgs boson should be

$$c_\pm = t_\beta s_\xi\left((2\lambda_6 - \lambda_7) + \lambda_3\eta_1 + \frac{\lambda_5\eta_2}{2}\right); \quad (34)$$

where

$$\eta_1 = c_\theta\frac{(\tilde{m}_1)_{12}}{(\tilde{m}_0)_{22}} - s_\theta\frac{(\tilde{m}_1)_{13}}{(\tilde{m}_0)_{33}} = 2(\lambda_3+\lambda_7)\left(\frac{c_\theta^2}{(\tilde{m}_0)_{22}} + \frac{s_\theta^2}{(\tilde{m}_0)_{33}}\right) + \frac{\lambda_5 s_{2\theta}}{2}\left(\frac{1}{(\tilde{m}_0)_{22}} - \frac{1}{(\tilde{m}_0)_{33}}\right); \quad (35)$$

$$\eta_2 = s_\theta\frac{(\tilde{m}_1)_{12}}{(\tilde{m}_0)_{22}} + c_\theta\frac{(\tilde{m}_1)_{13}}{(\tilde{m}_0)_{33}} = (\lambda_3+\lambda_7)s_{2\theta}\left(\frac{1}{(\tilde{m}_0)_{22}} - \frac{1}{(\tilde{m}_0)_{33}}\right) + \lambda_5\left(\frac{c_\theta^2}{(\tilde{m}_0)_{22}} + \frac{s_\theta^2}{(\tilde{m}_0)_{33}}\right). \quad (36)$$

We choose all the nine free parameters as nine observables in the Higgs sector: masses of four scalars m_h, m_2, m_3, and $m_{H^\pm}$; vacuum expected values v_1, v_2, ξ; and two mixing angles for neutral bosons. The mixing angles are represented as c_1 and c_2.

$$\mathcal{L}_{h_iVV} = c_i h_i\left(\frac{2m_W^2}{v}W_\mu^+ W^{\mu-} + \frac{m_Z^2}{v}Z_\mu Z^\mu\right). \quad (37)$$

The c_i just stands for the h_iVV vertex strength ratio compared with that in SM.[5] In the scalar sector, for nondegenerate neutral Higgs bosons, a quantity $K = c_1c_2c_3$ measures the CP-violation effects [49,50],[6] while in the Yukawa sector, the Jarlskog invariant J [30] measures that. In this scenario, to the leading order of $t_\beta s_\xi$, we have

$$K = c_1c_2c_3 = -s_\theta c_\theta(1+\eta_1)t_\beta s_\xi \propto t_\beta s_\xi. \quad (38)$$

In order to calculate J, we define matrix $\hat{C}$ as

$$\hat{C} \equiv [M_U M_U^\dagger, M_D M_D^\dagger]. \quad (39)$$

We can always choose a basis in which the diagonal elements of $\hat{C}$ are zero. Thus,

$$\hat{C} = \begin{pmatrix} 0 & C_3 & -C_2 \\ -C_3 & 0 & C_1 \\ C_2 & -C_1 & 0 \end{pmatrix} + i\begin{pmatrix} 0 & C_3^* & C_2^* \\ C_3^* & 0 & C_1^* \\ C_2^* & C_1^* & 0 \end{pmatrix} = (\text{Re}\hat{C} + i\text{Im}\hat{C}), \quad (40)$$

in which using Eqs. (27)–(28), to the leading order of $t_\beta s_\xi$, we have

$$\text{Re}\hat{C} = \frac{v^4c_\beta^4}{4}[Y_{u1}Y_{u1}^\dagger, Y_{d1}Y_{d1}^\dagger]; \quad (41)$$

$$\text{Im}\hat{C} = \frac{v^4c_\beta^4}{4}([Y_{u1}Y_{u2}^\dagger - Y_{u2}Y_{u1}^\dagger, Y_{d1}Y_{d1}^\dagger] + [Y_{u1}Y_{u1}^\dagger, Y_{d2}Y_{d1}^\dagger - Y_{d1}Y_{d2}^\dagger])t_\beta s_\xi \propto t_\beta s_\xi. \quad (42)$$

To the leading order of $t_\beta s_\xi$, the determinant

$$\det(i\hat{C}) \equiv 2J\prod_{i<j}(m_{U_i}^2 - m_{U_j}^2)\prod_{i<j}(m_{D_i}^2 - m_{D_j}^2) = C_1C_2C_3\left(\frac{C_1^*}{C_1} + \frac{C_2^*}{C_2} + \frac{C_3^*}{C_3}\right), \quad (43)$$

where $C_i^* \propto t_\beta s_\xi$; thus,

[5]There is a sum rule $c_1^2 + c_2^2 + c_3^2 = 1$ due to spontaneous electroweak symmetry breaking; thus, only two of the c_i are free, and c_1 here is just the c_V in (31).

[6]If at least two of the neutral bosons have degenerate mass, we can always perform a rotation among the neutral fields to keep $K = 0$.

$$J = \frac{\prod C_i \sum (C_i^*/C_i)}{\prod (m_{U_i}^2 - m_{U_j}^2) \prod (m_{D_i}^2 - m_{D_j}^2)} \propto t_\beta s_\xi. \quad (44)$$

According to the Eqs. (38), (44), and (22), we propose that the lightness of the Higgs boson and the smallness of *CP*-violation effects could be correlated through small $t_\beta s_\xi$ since both the Higgs mass m_h and the quantities K and J to measure *CP*-violation effects are proportional to $t_\beta s_\xi$ at the small $t_\beta s_\xi$ limit.

In the following two sections, we will study whether the Lee model is still viable to confront the current numerous high and low energy measurements. From Eq. (31), it is quite clear that couplings of discovered scalar boson differ from those in the SM, namely, the Lee model does not have a SM limit. Provided that the LHC obtained only a small portion of its designed integrated luminosity, there would be spacious room for the Lee model. In the long run, the LHC and future facilities have the great potential to discover/exclude the Lee model. We will discuss this part in Sec. V.

III. CONSTRAINTS FROM HIGH ENERGY PHENOMENA

In this model there are two more neutral bosons and one more charged boson pair comparing with the SM; these degree of freedoms may affect the physics at electroweak scale, and they could also be constrained by direct searches at the LHC. For the discovered boson, the SM predicts the decay branching ratios for a Higgs boson with mass 125.7 GeV in Table I. However, in the Lee model, the modified couplings will change the total width and branching ratios due to Eqs. (31)–(34), together with the production cross sections modified by (33) for gluon fusion and (31) for vector boson fusion and the associated production with vector bosons. Of course, this model may also affect top physics because the couplings between Higgs boson and top quark are not suppressed and it may also change the flavor-changing couplings especially for the top quark. Thus, it is necessary to discuss the constraints to this model from high energy phenomena.

A. Constraints on heavy neutral bosons

A heavy Higgs boson may decay to W^+W^-, $2Z_0$, $2h$, $t\bar{t}$ (for neutral bosons heavier than $2m_t \approx 346$ GeV), or H^+H^- (for light charged Higgs boson and a neutral boson heavier than $2m_{H^\pm}$). Based on the searches for the SM Higgs boson using diboson final state [51], masses and couplings of the other two heavier neutral Higgs bosons should be constrained by the data. For a neutral Higgs boson heavier than 350 GeV, the $t\bar{t}$ resonance search [52] may also give some constraints.

In this scenario, the total width of a heavy boson can be expressed as

$$\Gamma_i = \Gamma_{i,VV} + \Gamma_{i,\pm} + \Gamma_{i,2h} + \Gamma_{i,t\bar{t}}, \quad (45)$$

where $\Gamma_{i,VV}$, $\Gamma_{i,\pm}$, $\Gamma_{i,2h}$, $\Gamma_{i,t\bar{t}}$ correspond to massive gauge boson pairs, charged Higgs pair, neutral Higgs pair, and top quark pair final states, respectively. The partial decay width for a heavy neutral Higgs boson with mass m_i is

$$\frac{\Gamma_{i,VV}}{m_i} = \frac{3c_i^2}{16\pi}\left(\frac{m_i}{v}\right)^2 \quad (m_i \gg m_V); \quad (46)$$

$$\frac{\Gamma_{i,t\bar{t}}}{m_i} = \frac{3|c_{t,i}|^2}{8\pi}\left(\frac{m_t}{v}\right)^2 \sqrt{1-\frac{4m_t^2}{m_i^2}}\left(1-\frac{4m_t^2\cos^2(\arg(c_{t,i}))}{m_i^2}\right); \quad (47)$$

$$\frac{\Gamma_{i,\pm}}{m_i} = \frac{\lambda_{i,\pm}^2}{16\pi}\left(\frac{v}{M}\right)^2 \sqrt{1-\frac{4m_{H^\pm}^2}{m_i^2}}; \quad (48)$$

$$\frac{\Gamma_{i,hh}}{m_i} = \frac{\lambda_{i,hh}^2}{32\pi}\left(\frac{v}{M}\right)^2 \sqrt{1-\frac{4m_h^2}{m_i^2}} \quad (49)$$

in units of its mass. Here, we have the vertices

$$\lambda_{i,\pm} = \frac{1}{v}\frac{\partial^3 V}{\partial h_i \partial H^+ \partial H^-}, \qquad \lambda_{i,hh} = \frac{1}{v}\frac{\partial^3 V}{\partial h_i \partial h^2}. \quad (50)$$

The couplings $\lambda_{i,\pm}$, $\lambda_{i,hh} \sim \mathcal{O}(1)$.

The signal strength is defined as

$$\mu = \frac{\sigma}{\sigma_{\rm SM}} \cdot \frac{\Gamma_{i,VV}}{\Gamma_i} \cdot \frac{1}{{\rm Br}_{{\rm SM}(VV)}} \quad (51)$$

for a production channel. The $\sigma/\sigma_{\rm SM} \lesssim \mathcal{O}(1)$ for different channels. For a heavy Higgs boson with $m_i \leq 2m_t$, ${\rm Br}_{\rm SM}(VV)$ is very close to 1; while for $m_i > 2m_t$, ${\rm Br}_{\rm SM}(VV)$ has a minimal value of about 0.8 when $m_i \sim 500$ GeV. According to (46)–(49), we can estimate that for both $m_i \sim v$ and $m_i \gg v$, $\mu \sim \mathcal{O}(0.1$–$1)$.

Thus, according to the figures in [51], we have three types of typical choices for the mass of two heavy neutral Higgs particles in Table IV. (Here, we write the mass of the lighter boson m_2 and the heavier one m_3.)

TABLE IV. Typical choices for the masses of the two heavy neutral scalars.

Case	Allowed m_2 (GeV)	Allowed m_3 (GeV)
I	$\lesssim$300	$\lesssim$300
II	$\lesssim$300	$\gtrsim$700
III	$\gtrsim$700	$\gtrsim$700

B. Constraints due to oblique parameters

Since the discovery of the new boson, there are new electroweak fits for the standard model [18]. Choosing $m_{t,\mathrm{ref}} = 173$ GeV and $m_{h,\mathrm{ref}} = 126$ GeV, the oblique parameters [19] are

$$S = 0.03 \pm 0.10, \quad T = 0.05 \pm 0.12, \quad U = 0.03 \pm 0.10,$$
$$R_{ST} = +0.89, \quad R_{SU} = -0.54, \quad R_{TU} = -0.83, \tag{52}$$

with R being the correlation coefficient between two quantities; or

$$S = 0.05 \pm 0.09, \quad T = 0.08 \pm 0.07, \quad R = +0.91, \tag{53}$$

with fixed $U = 0$, where R is the correlation coefficient between S and T. The basic *Mathematica* code to draw the S-T ellipse can be found on the webpage [53].[7] The contribution to S and T parameters due to multi-Higgs doublets was calculated in [54] (see the formulas in [49]).

$$\Delta T = \frac{1}{16\pi s_W^2 m_W^2}\left[\sum_{i=1}^{3}(1-c_i^2)F(m_{H^\pm}^2, m_i^2) - c_1^2 F(m_2^2, m_3^2) - c_2^2 F(m_3^2, m_1^2) - c_3^2 F(m_1^2, m_2^2)\right.$$
$$\left. + 3\sum_{i=1}^{3} c_i^2 (F(m_Z^2, m_i^2) - F(m_W^2, m_i^2)) - 3(F(m_Z^2, m_{h,\mathrm{ref}}^2) - F(m_W^2, m_{h,\mathrm{ref}}^2))\right]; \tag{54}$$

$$\Delta S = \frac{1}{24\pi}\left[(1-2s_W^2)^2 G(z_\pm, z_\pm) + c_1^2 G(z_2, z_3) + c_2^2 G(z_3, z_1) + c_3^2 G(z_1, z_2)\right.$$
$$\left. + \sum_{i=1}^{3}\left(c_i^2 H(z_i) + \ln\left(\frac{m_i^2}{m_{H^\pm}^2}\right)\right) - H\left(\frac{m_{h,\mathrm{ref}}^2}{m_Z^2}\right) - \ln\left(\frac{m_{h,\mathrm{ref}}^2}{m_{H^\pm}^2}\right)\right]; \tag{55}$$

where c_i is the rate of the $h_i V_\mu V^\mu$ coupling to that in the SM (c_1 represents the above-mentioned c_V) and $\sum c_i^2 = 1$. $m_{h,\mathrm{ref}} = m_1 = 126$ GeV is the reference point for Higgs boson, $z_\pm = (m_{H^\pm}/m_Z)^2$ and $z_i = (m_i/m_Z)^2$. The functions F, G, H read (following the formulas in [49])

$$F(x,y) = \frac{x+y}{2} - \frac{xy}{x-y}\ln\left(\frac{x}{y}\right); \tag{56}$$

$$G(x,y) = -\frac{16}{3} + 5(x+y) - 2(x-y)^2$$
$$+ 3\left(\frac{x^2+y^2}{x-y} + y^2 - x^2 + \frac{(x-y)^3}{3}\right)\ln\left(\frac{x}{y}\right)$$
$$+ (1 - 2(x+y) + (x-y)^2)$$
$$\times f(x+y-1, 1-2(x+y)+(x-y)^2); \tag{57}$$

$$H(x) = -\frac{79}{3} + 9x - 2x^2$$
$$+ \left(-10 + 18x - 6x^2 + x^3 - 9\frac{x+1}{x-1}\right)\ln x$$
$$+ (12 - 4x + x^2) f(x, x^2 - 4x); \tag{58}$$

where

$$f(x,y) = \begin{cases} \sqrt{y}\ln\left|\frac{x-\sqrt{y}}{x+\sqrt{y}}\right|, & y \geq 0; \\ 2\sqrt{-y}\arctan\left(\frac{\sqrt{-y}}{x}\right), & y < 0. \end{cases} \tag{59}$$

At removable singularities the functions are defined as the limit.

The parameter U is usually small so that we fix $U = 0$ from now on. We take the benchmark points according to the cases in Table IV. We show the contours in Figs. 1–3 for the cases listed in Table IV in the last section. Throughout the paper, the region outside the green area is excluded at 68% C.L. and the region outside the yellow area is excluded at 95% C.L. First, for case I, we take $m_2 = 280$ GeV and $m_3 = 300$ GeV. The typical values for the left diagram in Fig. 1 are $c_1^2 = 0.2$, $c_2^2 = c_3^2 = 0.4$. Here, the blue and red lines refer to 86 GeV $< m_{H^\pm} <$ 126 GeV and 312 GeV $< m_{H^\pm} <$ 350 GeV, respectively. For the right diagram, $c_1^2 = 0.25$, $c_2^2 = 0.4$, $c_3^2 = 0.35$, and

[7] Assuming Gaussian distribution, the second $\Delta\chi^2$ should be 6.0 instead of 6.8 in the code. See the 36th chapter (statistics) of the reviews in PDG [28], in for its 2014 updated version please see the 38th chapter instead.

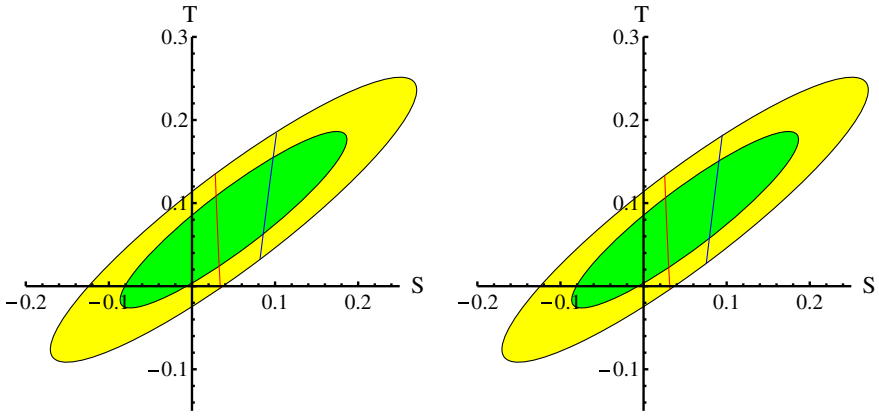

FIG. 1 (color online). S-T ellipse for case I, $m_2 = 280$ GeV and $m_3 = 300$ GeV.

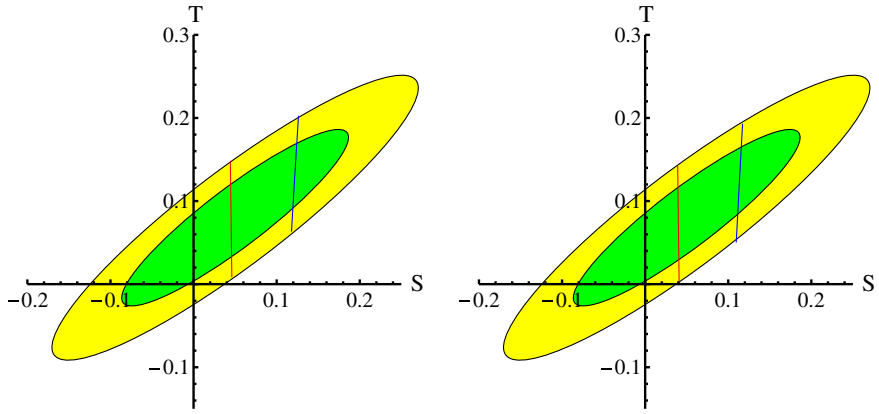

FIG. 2 (color online). S-T ellipse for case II, $m_2 = 300$ GeV and $m_3 = 700$ GeV.

the blue and red lines refer to 94 GeV $< m_{H^\pm} <$ 136 GeV and 312 GeV $< m_{H^\pm} <$ 351 GeV, respectively.

Second, for case II, we take $m_2 = 300$ GeV and $m_3 = 700$ GeV. The typical values for the left diagram in Fig. 2 are $c_1^2 = 0.2$, $c_2^2 = 0.5$, $c_3^2 = 0.3$. Here, the blue and red lines refer to 127 GeV $< m_{H^\pm} <$ 149 GeV and 580 GeV $< m_{H^\pm} <$ 600 GeV, respectively. For the right diagram, $c_1^2 = c_3^2 = 0.25$, $c_2^2 = 0.5$, and the blue and red lines refer to 141 GeV $< m_{H^\pm} <$ 163 GeV and 598 GeV $< m_{H^\pm} <$ 618 GeV, respectively.

Third, for case III, we take $m_2 = 700$ GeV and $m_3 = 750$ GeV. The typical values for the left diagram in Fig. 3 are $c_1^2 = 0.2$, $c_2^2 = c_3^2 = 0.4$. Here, the blue and red lines refer to 218 GeV $< m_{H^\pm} <$ 235 GeV and

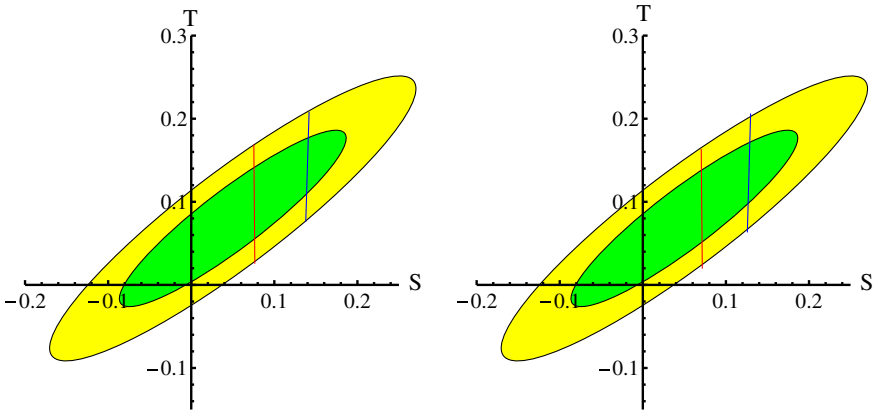

FIG. 3 (color online). S-T ellipse for case III, $m_2 = 700$ GeV and $m_3 = 750$ GeV.

748 GeV $< m_{H^\pm} <$ 765 GeV, respectively. For the right diagram, $c_1^2 = 0.25$, $c_2^2 = 0.4$, $c_3^2 = 0.35$, and the blue and red lines refer to 250 GeV $< m_{H^\pm} <$ 269 GeV and 749 GeV $< m_{H^\pm} <$ 767 GeV, respectively.

In type II 2HDM the charged Higgs boson should be heavier than 360 GeV [55,56] mainly due to the constraint from inclusive $b \to s\gamma$ process. However, in other models, there are no such strict constraints. Direct searches by LEP told us that the charged Higgs boson should be heavier than 78.6 GeV [57]. In cases I–II above, a light (around 100–200 GeV) charged Higgs boson is allowed, while in case III the charged Higgs boson cannot be lighter than about 250 GeV. In cases I and III, a charged Higgs boson with the mass near the heavy neutral bosons is allowed, while in case II a heavy charged Higgs boson must be lighter than the heaviest neutral scalar.

C. Constraints due to signal strengths

In Tables II–III, for a certain channel, the signal strength is defined as

$$\mu_f = \frac{\sigma \cdot \mathrm{Br}_f}{(\sigma \cdot \mathrm{Br}_f)_{\mathrm{SM}}} = \frac{\sigma}{\sigma_{\mathrm{SM}}} \cdot \frac{\Gamma_f}{\Gamma_{f,\mathrm{SM}}} \cdot \frac{\Gamma_{\mathrm{tot,SM}}}{\Gamma_{\mathrm{tot}}}, \tag{60}$$

in which $\sigma/\sigma_{\mathrm{SM}} = |c_t'|^2$ for gluon fusion processes and $\sigma/\sigma_{\mathrm{SM}} = c_V^2$ for VBF processes and associated productions with a gauge boson. For decays without interference, we simply have $\Gamma_f/\Gamma_{f,\mathrm{SM}} = |c_f|^2$ such as for $f = V$, b, τ, while for the two photons final state, we have [6,22]

$$\frac{\Gamma_{\gamma\gamma}}{\Gamma_{\gamma\gamma,\mathrm{SM}}} = \left| \frac{(4/3)c_t' \mathcal{A}_{1/2}(x_t) + c_V \mathcal{A}_1(x_W) + (c_\pm v^2/2m_{H^\pm}^2)\mathcal{A}_0(x_\pm)}{(4/3)\mathcal{A}_{1/2}(x_t) + \mathcal{A}_1(x_W)} \right|^2, \tag{61}$$

in which $x_i = m_h^2/4m_i^2$ for $i = t$, W, $H^\pm$. The loop integration functions are

$$\mathcal{A}_0(x) = \frac{1}{x^2}(x - f(x)) \tag{62}$$

$$\mathcal{A}_{1/2}(x) = -\frac{2}{x^2}(x + (x-1)f(x)) \tag{63}$$

$$\mathcal{A}_1(x) = \frac{1}{x^2}(2x^2 + 3x + 3(2x-1)f(x)) \tag{64}$$

for scalar, fermion, and vector boson loops, respectively, and

$$f(x) = \begin{cases} \arcsin^2\sqrt{x}, & x \le 1; \\ -\frac{1}{4}\left(\ln\left(\frac{1+\sqrt{1-1/x}}{1-\sqrt{1-1/x}}\right) - \pi i\right)^2, & x > 1. \end{cases} \tag{65}$$

In a spontaneous CP-violation model, c_t' (together with other c_f for fermions) can be complex while c_V and $c_\pm$ must be real. Notice that all the c_V, $c_\pm$, c_b, and c_τ are the same as those in (31)–(34), but c_t should be modified to c_t' as

$$c_t' = \mathrm{Re}(c_t) + i\frac{\mathcal{B}_{1/2}(m_h^2/4m_t^2)}{\mathcal{A}_{1/2}(m_h^2/4m_t^2)}\mathrm{Im}(c_t) \tag{66}$$

in which the function

$$\mathcal{B}_{1/2}(x) = -\frac{2f(x)}{x}. \tag{67}$$

Thus, defining $\alpha_t \equiv \arg(c_t)$ and $\alpha_t' \equiv \arg(c_t')$, numerically we have

$$\alpha_t' = \arctan(1.52\tan\alpha_t), \qquad |c_t'| = |c_t|\sqrt{1 + 1.31\sin^2\alpha_t}. \tag{68}$$

Assuming there is no unknown decay channel that contributes several percentages or more to the total width, we can estimate that

$$\frac{\Gamma_{\mathrm{tot}}}{\Gamma_{\mathrm{tot,SM}}} = 0.57|c_b|^2 + 0.25c_V^2 + 0.06|c_\tau|^2 + 0.03|c_c|^2 + 0.09|c_t'|^2 \tag{69}$$

according to Table I.

Define the χ^2

$$\chi^2 = \sum_{i,f}\left(\frac{\mu_{i,f,\mathrm{obs}} - \mu_{i,f,\mathrm{pre}}}{\sigma_{i,f}}\right)^2, \tag{70}$$

where $i =$ VBF, ggF, VH and $f = \gamma\gamma$, WW^*, ZZ^*, $\tau^+\tau^-$ at a detector (CMS or ATLAS). The $\mu_{i,f,\mathrm{obs(pre)}}$ are the observed (predicted) signal strength for the production channel i and final state f. We ignored all correlation coefficients between channels since they are small.

Numerically, we find that the minimal χ^2 is not sensitive to the charged Higgs mass since the scalar loop contributes less than the top and W loop in the $\gamma\gamma$ decay channel. Thus, we take the benchmark point as $m_{H^\pm} = 150$ GeV. For six degrees of freedom, parameter space with $\chi^2 \le 7.0$ is allowed at 68% C.L. and $\chi^2 \le 12.6$ is allowed at 95% C.L. For both CMS and ATLAS data, the minimal χ^2 is very sensitive to c_V and c_t', since they give dominant contributions to most production cross sections and partial decay widths; it is sensitive to c_b as well since the total

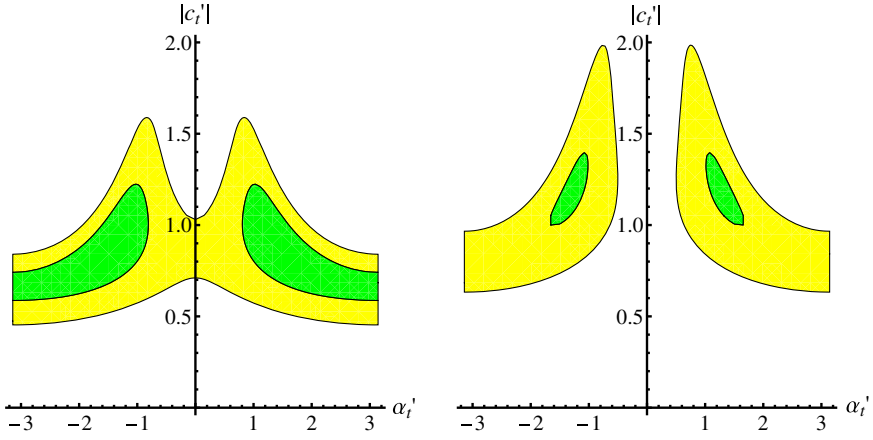

FIG. 4 (color online). Allowed $|c_t'| - \alpha_t'$ contour when taking $c_V = 0.4$, $c_\pm = 0.2$, and $|c_\tau| = 0.8$ for CMS data. $|c_b| = 0.1$ for the left figure and $|c_b| = 0.4$ for the right figure.

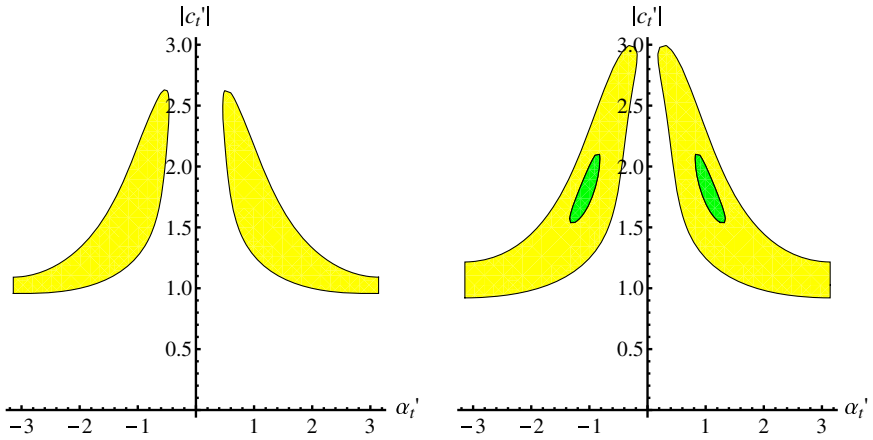

FIG. 5 (color online). Allowed $|c_t'| - \alpha_t'$ contour when taking $c_V = 0.4$, $c_\pm = 0.2$, and $|c_b| = 0.7$ for CMS data. $|c_\tau| = 0.8$ for the left figure and $|c_\tau| = 1.3$ for the right figure.

width is sensitive to $|c_b|$. With the CMS data, we have $c_V \geq 0.22$; and with the ATLAS data, we have $c_V \geq 0.31$, both at 95% C.L. So $c_V = 0.5$ is a good benchmark point as we have chosen in the last section, and it will also be taken around this point in later analysis. The χ^2 is not very sensitive to $|c_\tau|$ and $c_\pm$, as both of them contribute to only one channel, and the charged Higgs loop contributes less in the $\gamma\gamma$ decay channel. Thus, for most analysis we do not discuss these two parameters carefully.

For the CMS data, when $c_V \sim 0.5$, the $\chi^2_{\rm min} \approx 2$. The data favor smaller $|c_b|$ but the minimal value of χ^2 changes little as c_b varies, since the points are far away from the 95% allowed boundary $c_V = 0.22$. Figures 4–6 show CMS allowed $|c_t'|$ and $\alpha_t' \equiv \arg(c_t')$ for some benchmark points.[8]

In Figs. 4–5, we choose $c_V = 0.4$. Fixing $c_\pm = 0.2$ and $|c_\tau| = 0.8$, and taking $|c_b| = 0.1$, 0.4, 0.7, we have the three figures in Figs. 4–5. The best fit point for $|c_t|$ has positive correlation with $|c_b|$. For larger $|c_b|$, the best fit point for $|c_\tau|$ increases as well; thus, in the right figure in Fig. 5 we set $|c_\tau| = 1.3$ and get a better fitting result.

In Figure 6, we have $c_V = 0.5$. Fixing $c_\pm = 0.2$ and $|c_\tau| = 0.9$, and taking $|c_b| = 0.1$, 0.3, 0.5, 0.7, we get the four figures. The fitting results are less sensitive to $|c_\tau|$ than in Figs. 4–5, and the best fit point for $|c_t'|$ has positive correlation with $|c_b|$ as well. Usually $\alpha_t' \sim 0$ is disfavored while for smaller $|c_b|$ and larger c_V any α_t' is allowed. For each case, the best fit point is about $|\alpha_t'| \sim 1.2$.

For the ATLAS data, when $c_V \sim 0.5$, the $\chi^2_{\rm min} \approx 7$, which is near the 1σ allowed boundary. The data favor smaller $|c_b|$ as well just like the CMS case. Figures 7–8 show ATLAS allowed $|c_t'|$ and $\alpha_t' \equiv \arg(c_t')$ for some benchmark points.

In Fig. 7 we show the allowed regions for c_t'. Fixing $c_V = 0.5$, $c_\pm = 0.4$, and $|c_\tau| = 0.7$, choosing $|c_b| = 0.2$, 0.4, we have the two figures. In Fig. 8, fixing $c_V = 0.6$,

[8]In this paper, the benchmark points are close to the best fit points for a certain case; thus, the allowed regions are typical enough.

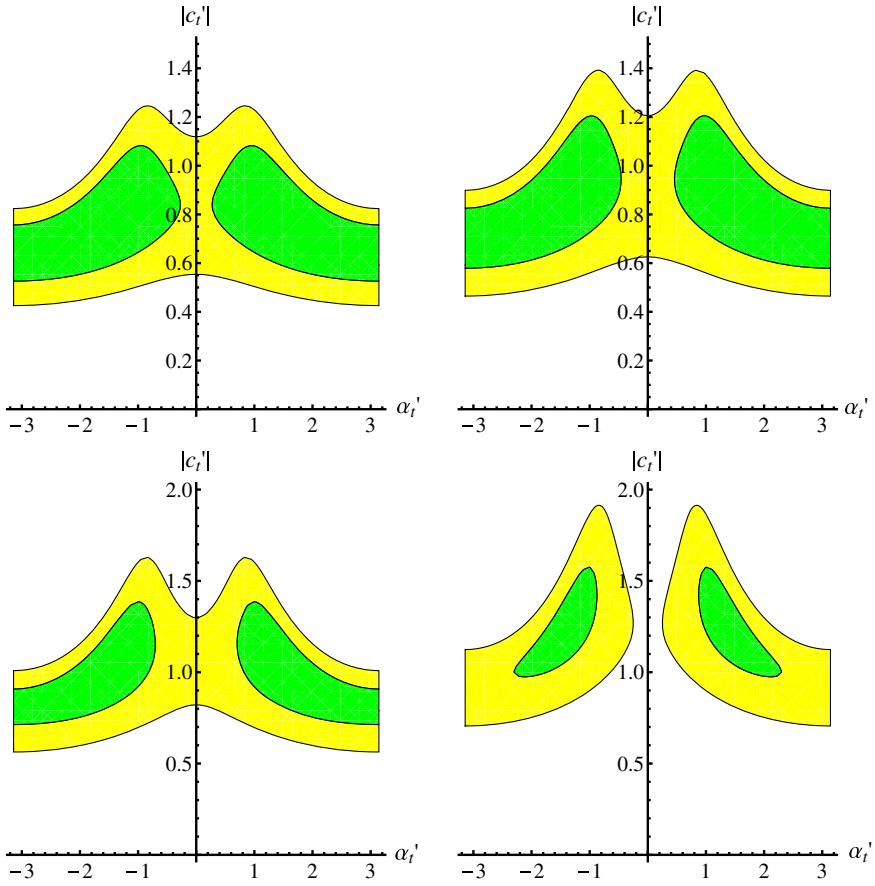

FIG. 6 (color online). Allowed $|c_t'| - \alpha_t'$ contour when taking $c_V = 0.5$, $c_\pm = 0.2$, and $|c_\tau| = 1$ for CMS data. The four figures correspond to $|c_b| = 0.1$, 0.3, 0.5, 0.7, respectively.

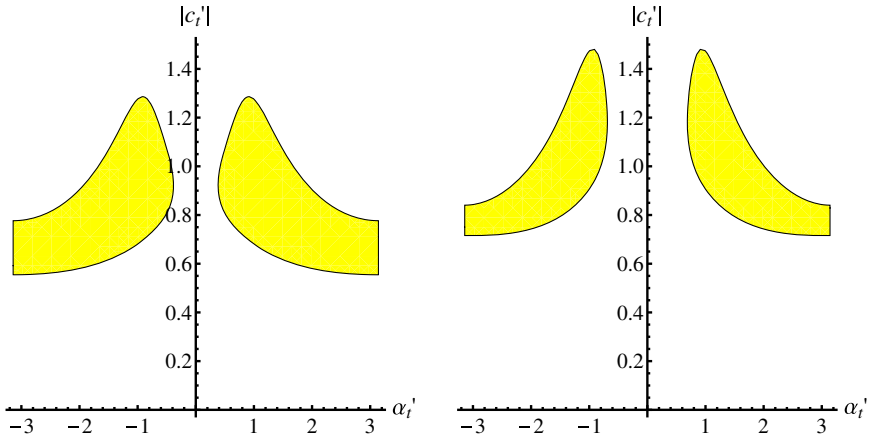

FIG. 7 (color online). Allowed $|c_t'| - \alpha_t'$ contour when taking $c_V = 0.5$, $c_\pm = 0.4$, and $|c_\tau| = 0.7$ for ATLAS data. The left and right figures correspond to $|c_b| = 0.2$ and $|c_b| = 0.4$, respectively.

$c_\pm = 0.4$, and $|c_\tau| = 0.8$, and taking $|c_b| = 0.1$, 0.3, 0.5, 0.7, we have the four figures. Usually, $\alpha_t' \sim 0$ is disfavored while for smaller $|c_b|$ and larger c_V any α_t' is allowed. The best fit points for α_t' are around $|\alpha_t'| \sim 1.2$; all these behaviors are similar to the results from CMS data.

For both CMS and ATLAS data, smaller $|c_b|$ is favored. In most cases, the best fit points for $|c_t'|$, $|c_\tau|$ are around 1, and $c_\pm \sim \mathcal{O}(0.1)$. The fitting results for α_t' favor smaller $|\alpha_t'|(\sim 1.2)$ by both data for most $|c_b|$ inputs. We also have the χ^2 for the SM as

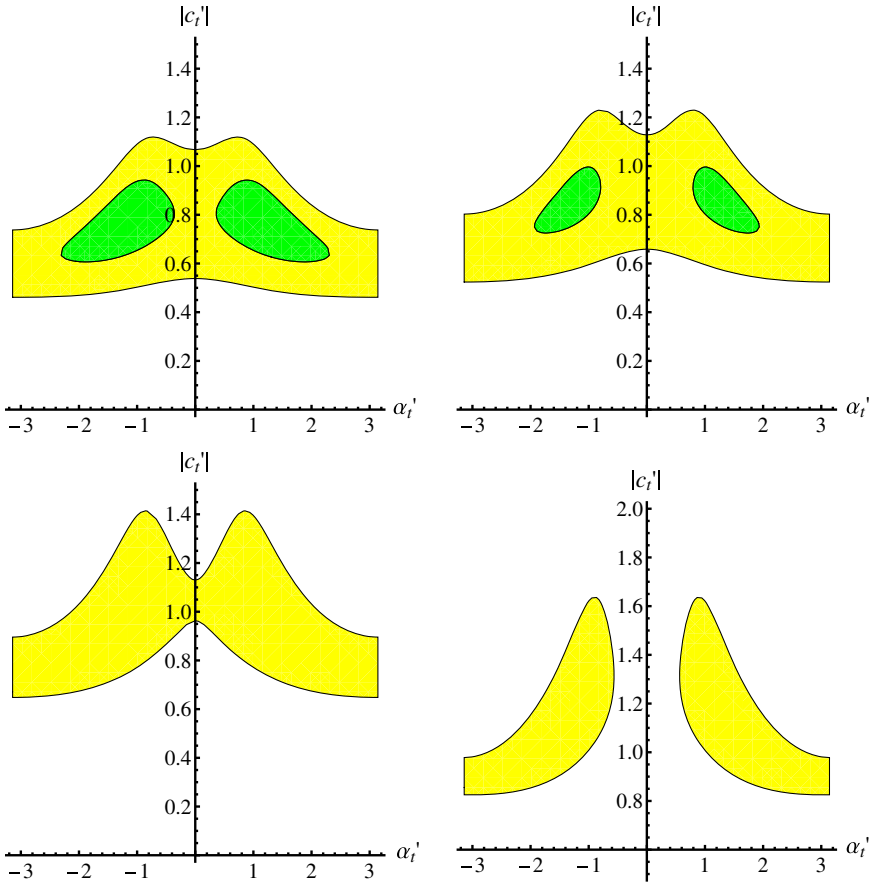

FIG. 8 (color online). Allowed $|c_t'| - \alpha_t'$ contour when taking $c_V = 0.6$, $c_\pm = 0.4$, and $|c_\tau| = 0.8$ for ATLAS data. The four figures correspond to $|c_b| = 0.1$, 0.3, 0.5, 0.7, respectively.

$$\chi^2_{\mathrm{SM,CMS}} = 2.4, \qquad \chi^2_{\mathrm{SM,ATLAS}} = 3.7 \tag{71}$$

close to the minimal χ^2 for the Lee model we discussed in this paper. So the Lee model can fit the current data as well as those in the SM.

D. Same sign top production

We put no additional symmetries in the Yukawa sector to avoid tree-level FCNC; thus, the model must be constrained by processes including flavor-changing interactions. The tree-level FCNC for up-type quarks will lead to same sign top quarks production at the LHC. An upper limit at 95% C.L. was given as [58]

$$\sigma_{tt} < 0.37 \text{ pb} \tag{72}$$

by the CMS group with an integrated luminosity 19.5 fb^{-1} at $\sqrt{s} = 8$ TeV.

In this model, we can write the interaction that can induce same sign top quark production at the LHC as

$$\mathcal{L}_{I,tuh} = -\frac{1}{\sqrt{2}}\bar{t}(\xi_{1tu} + \xi_{2tu}\gamma^5)uh + \text{H.c.} \tag{73}$$

The lightest neutral boson gives the dominant contribution when the effect couplings are similar. A direct calculation gives

$$\sigma_{tt} = \int dx_1 dx_2 f_u(x_1) f_u(x_2)\sigma_0 \tag{74}$$

in which

$$\sigma_0 = \frac{|\xi_{tu}|^4\beta_t}{64\pi s_0}\int_{-1}^{1} dc_\theta \left[\left(\frac{1-\beta_t c_\theta}{1+\beta_t^2+4m_h^2/s_0-2\beta_t c_\theta}\right)^2 + \left(\frac{1+\beta_t c_\theta}{1+\beta_t^2+4m_h^2/s_0+2\beta_t c_\theta}\right)^2 - \frac{1+\beta_t^2 c_\theta^2-2\beta_t^2}{(1+\beta_t^2+4m_h^2/s_0)^2-4\beta_t^2 c_\theta^2}\right], \tag{75}$$

if $\xi_{1tu}\xi^*_{2tu} + \xi_{2tu}\xi^*_{1tu} = 0$ where s_0 is the square of energy in the frame of momentum center of two partons (both u quarks). $\beta_t = \sqrt{1-4m_t^2/s_0}$ is the velocity of a top quark and θ is the radiative angle in the same frame and $|\xi_{tu}| = \sqrt{|\xi_{1tu}|^2 + |\xi_{2tu}|^2}$. Using the MSTW2008 PDF

[59] and comparing with (72), we can estimate that $|\xi_{tu}| \lesssim 0.4$.

E. Top rare decays

In this model, the FCNC interactions including up-type quarks will induce rare decay processes of top quark, such as $t \to ch$ and $t \to uh$, usually with a larger decay rate than that in the SM. When the charged Higgs boson is lighter than the top quark, there will be a new decay channel $t \to H^+ b$ as well. Direct search results at $\sqrt{s} = 8$ TeV by CMS at the LHC gave the top pair production cross section [60] $\sigma_{t\bar{t}} = (237 \pm 13)$ pb assuming $m_t = 173$ GeV and $\mathrm{Br}(t \to bW) = 1$, while theoretical calculation predicts that [61] $\sigma_{t\bar{t},\mathrm{pre}} = (246^{+9}_{-11})$ pb. Assuming there are no effects beyond the SM during the production of top pair, these results can constrain the top rare decay (all channels except bW) branching ratio

$$\mathrm{Br}_{t,\mathrm{rare}} = 1 - \mathrm{Br}(t \to bW) < 7.4\% \tag{76}$$

at 95% C.L.

For the rare decay processes above, the interactions can be written as

$$\mathcal{L}_{I,tch} = -\frac{1}{\sqrt{2}}\bar{t}(\xi_{1tc} + \xi_{2tc}\gamma^5)ch + \mathrm{H.c.} \tag{77}$$

$$\mathcal{L}_{I,tbH^+} = -\bar{t}(\xi_{1tb} + \xi_{2tb}\gamma^5)bH^+ + \mathrm{H.c.} \tag{78}$$

together with (73). Direct calculations give the decay rates

$$\Gamma_{hu(hc)} = \frac{|\xi_{tu(tc)}|^2 m_t}{32\pi}\left(1 - \frac{m_h^2}{m_t^2}\right)^2 \tag{79}$$

$$\Gamma_{H^+b} = \frac{|\xi_{tb}|^2 m_t}{16\pi}\left(1 - \frac{m_{H^\pm}^2}{m_t^2}\right)^2, \tag{80}$$

where $|\xi_{ti}| = \sqrt{|\xi_{1ti}|^2 + |\xi_{2ti}|^2}$.

Direct search for $t \to c(u)h \to c(u)\gamma\gamma$ decays [62] at ATLAS gives the bound for branching ratios

$$\mathrm{Br}(t \to ch) + \mathrm{Br}(t \to uh) < 0.79\% \cdot \left(\frac{\mathrm{Br}(h \to \gamma\gamma)_{\mathrm{SM}}}{\mathrm{Br}(h \to \gamma\gamma)}\right) \tag{81}$$

TABLE V. Constraints on the $t \to bH^+ \to b\tau^+\nu(c\bar{s})$ from direct searches for light charged Higgs boson (lighter than top quark).

Process ($H^+ \to f$)	Charged Higgs mass (GeV)	$\mathrm{Br}(t \to bH^+ \to bf)$ (95% C.L.)
$H^+ \to c\bar{s}$(ATLAS)	90–150	< (1.2%–5.1%)
$H^+ \to \tau^+\nu$(ATLAS)	90–160	< (0.8%–3.4%)
$H^+ \to \tau^+\nu$(CMS)	80–160	< (1.9%–4.1%)
$H^+ \to c\bar{s}$(CMS)	90– 160	< (1.7%–7.0%)

at 95% C.L., which leads to

$$\sqrt{|\xi_{tu}|^2 + |\xi_{tc}|^2} < 0.16\kappa, \quad \text{where}$$
$$\kappa = \sqrt{\frac{\mathrm{Br}(h \to \gamma\gamma)_{\mathrm{SM}}}{\mathrm{Br}(h \to \gamma\gamma)}} \sim \mathcal{O}(1) \tag{82}$$

and $\kappa = 1$ in the SM. For most cases it is a stronger constraint on $|\xi_{tu}|$ than that in the same sign top production process, but they are of the same order. A similar measurement by CMS [63] gives a 95% upper limit $\mathrm{Br}(t \to ch) < 0.56\%$; hence, $|\xi_{tc}| < 0.14$ with the combination of Higgs boson decaying to diphoton or multileptons assuming the SM decay branching ratios of Higgs boson. If we allow different branching ratios into the SM, the constraints on this coupling is still of that order. Adopting the Cheng-Sher ansatz [43], we have

$$\frac{|\xi_{tc}|v}{\sqrt{2m_t m_c}} \lesssim 1.5, \quad \text{and} \quad \frac{|\xi_{tu}|v}{\sqrt{2m_t m_u}} \lesssim 44 \tag{83}$$

assuming SM branching ratios of Higgs boson. For other branching ratios, the constraints are of the same order.

Direct searches for $t \to bH^+ \to b\tau^+\nu_\tau(c\bar{s})$ at ATLAS [64] for 90 GeV $< m_{H^\pm} <$ 160(150) GeV and at CMS [65] for 80 GeV $< m_{H^\pm} <$ 160 GeV gave the results in Table V. These results lead to the upper limits region on $|\xi_{tb}|$ at 95% C.L. as

$$|\xi_{tb}| < \begin{cases} (0.15\text{–}0.59)/\sqrt{\mathrm{Br}(\tau\nu)}, & (\mathrm{CMS}, 80\ \mathrm{GeV} < m_{H^\pm} < 160\ \mathrm{GeV}); \\ (0.15\text{–}1.12)/\sqrt{\mathrm{Br}(c\bar{s})}, & (\mathrm{CMS}, 90\ \mathrm{GeV} < m_{H^\pm} < 160\ \mathrm{GeV}); \\ (0.13\text{–}0.45)/\sqrt{\mathrm{Br}(\tau\nu)}, & (\mathrm{ATLAS}, 90\ \mathrm{GeV} < m_{H^\pm} < 160\ \mathrm{GeV}); \\ (0.19\text{–}0.27)/\sqrt{\mathrm{Br}(c\bar{s})}, & (\mathrm{ATLAS}, 90\ \mathrm{GeV} < m_{H^\pm} < 150\ \mathrm{GeV}). \end{cases} \tag{84}$$

TABLE VI. Constraints on the tbH^+ vertex coupling $|\xi_{tb}|$ for some typical mass of the charged Higgs boson.

Mass (GeV)	100	120	150
CMS($\tau\nu$)	$0.17/\sqrt{\mathrm{Br}(\tau\nu)}$	$0.20/\sqrt{\mathrm{Br}(\tau\nu)}$	$0.38/\sqrt{\mathrm{Br}(\tau\nu)}$
CMS($c\bar{s}$)	$0.15/\sqrt{\mathrm{Br}(c\bar{s})}$	$0.16/\sqrt{\mathrm{Br}(c\bar{s})}$	$0.43/\sqrt{\mathrm{Br}(c\bar{s})}$
ATLAS($\tau\nu$)	$0.16/\sqrt{\mathrm{Br}(\tau\nu)}$	$0.12/\sqrt{\mathrm{Br}(\tau\nu)}$	$0.25/\sqrt{\mathrm{Br}(\tau\nu)}$
ATLAS($c\bar{s}$)	$0.17/\sqrt{\mathrm{Br}(c\bar{s})}$	$0.16/\sqrt{\mathrm{Br}(c\bar{s})}$	$0.27/\sqrt{\mathrm{Br}(c\bar{s})}$

For some typical mass of charged Higgs boson (which are allowed for some cases in the S-T ellipse tests) we have the upper limits of $|\xi_{tb}|$ in Table VI. From all the direct searches for top decays, we must have a relation

$$\mathrm{Br}(t\to hc)+\mathrm{Br}(t\to hu)+\mathrm{Br}(t\to bH^+)<7.4\% \quad (85)$$

according to (76) at 95% C.L. as well.

IV. CONSTRAINTS FROM LOW ENERGY PHENOMENA

The Lee model we discussed in this paper contains additional sources of *CP* violation and tree-level FCNC interactions; therefore, they will affect many kinds of low energy phenomena, especially for the *CP*-violation observables and the FCNC processes. For the *CP*-violation observables, we will focus on the constraints from the EDMs of electron and neutron [66]. For the constraints on FCNC interactions, we will focus on the mesonic measurements.

A. Constraints due to EDM and strong *CP* phase

Direct searches of the EDM for electron (d_e) and neutron (d_n) are given as [34,67]

$$\begin{aligned} d_e &= (-2.1\pm 4.5)\times 10^{-29} e\,\mathrm{cm} \\ d_n &= (0.2\pm 1.7)\times 10^{-26} e\,\mathrm{cm}, \end{aligned} \quad (86)$$

which will constrain the corresponding *CP*-violation interactions.

The effective interaction for electrons can be written as [66]

$$\mathcal{L}_{e,\mathrm{EDM}} = -\frac{id_e}{2}\bar{e}\sigma^{\mu\nu}\gamma^5 e F_{\mu\nu}, \quad (87)$$

where d_e is the EDM for electrons. In our scenario, the dominant contribution to electron EDM should be due to the two-loop Barr-Zee–type diagrams [68,69] involving the lightest scalar as follows:

$$\begin{aligned} \frac{d_e}{e} &= \left(\frac{d_e}{e}\right)_{W^\pm} + \left(\frac{d_e}{e}\right)_{t} + \left(\frac{d_e}{e}\right)_{H^\pm} \\ &= \frac{2\sqrt{2}\alpha_{em}G_F m_e}{(4\pi)^3}\left(-c_V \mathrm{Im}(c_e) J_1(m_W,m_h) + \frac{8}{3}\mathrm{Re}(c_e)\mathrm{Im}(c_t) J_{1/2}(m_t,m_h)\right. \\ &\quad \left. + \frac{8}{3}\mathrm{Im}(c_e)\mathrm{Re}(c_t) J'_{1/2}(m_t,m_h) - c_\pm \mathrm{Im}(c_e) J_0(m_{H^\pm},m_h)\right), \end{aligned} \quad (88)$$

in which the loop integration functions J_1 come from the W loop, $J_{1/2}(J'_{1/2})$ comes from the top loop, and J_0 comes from the charged scalar loop. The analytical expressions are [69]

$$\begin{aligned} J_1(m_W,m_h) = -\frac{m_W^2}{m_h^2}\left(\left(5-\frac{m_h^2}{2m_W^2}\right) I_1(m_W,m_h)\right. \\ \left. + \left(3+\frac{m_h^2}{2m_W^2}\right) I_2(m_W,m_h)\right); \end{aligned} \quad (89)$$

$$J_{1/2}(m_t,m_h) = -\frac{m_t^2}{m_h^2} I_1(m_t,m_h); \quad (90)$$

$$J'_{1/2}(m_t,m_h) = -\frac{m_t^2}{m_h^2} I_2(m_t,m_h); \quad (91)$$

$$J_0(m_{H^\pm},m_h) = -\frac{v^2}{2m_h^2}\left(I_1(m_{H^\pm},m_h) - I_2(m_{H^\pm},m_h)\right); \quad (92)$$

where

$$\begin{aligned} I_1(m_1,m_2) &= \int_0^1 dz \frac{m_2^2}{m_1^2 - m_2^2 z(1-z)} \ln\left(\frac{m_2^2 z(1-z)}{m_1^2}\right); \\ I_2(m_1,m_2) &= \int_0^1 dz \frac{m_2^2(1-2z(1-z))}{m_1^2 - m_2^2 z(1-z)} \ln\left(\frac{m_2^2 z(1-z)}{m_1^2}\right). \end{aligned} \quad (93)$$

Numerically, the contribution from charged Higgs loop is usually small comparing with the W and top loop, especially for heavy charged Higgs bosons. As a benchmark point, take $m_{H^\pm} = 150$ GeV; we have

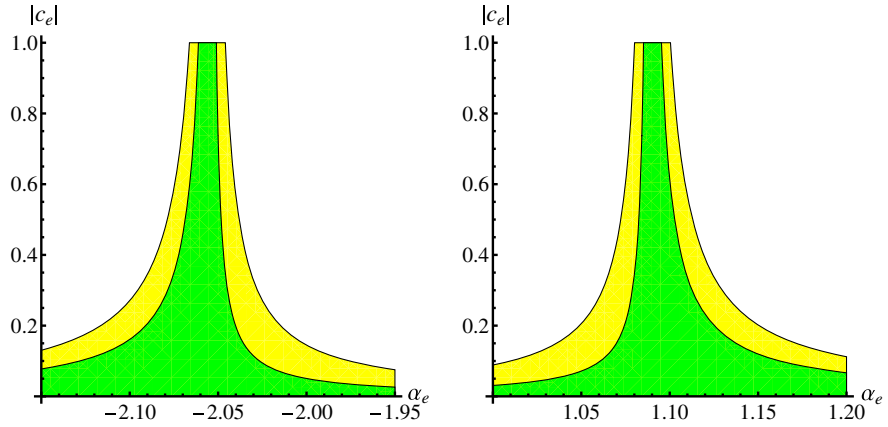

FIG. 9 (color online). Constraints on c_e taking $\alpha_t = 1.0$.

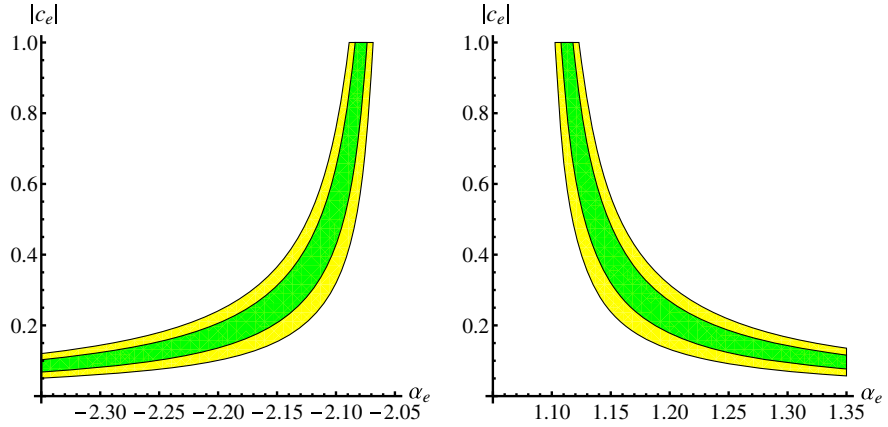

FIG. 10 (color online). An example of modified constraints by heavy neutral scalars.

$$d_e = [-(14.0c_V + 1.28c_\pm)\mathrm{Im}(c_e) + 6.53\mathrm{Re}(c_t)\mathrm{Im}(c_e) + 9.32\mathrm{Re}(c_e)\mathrm{Im}(c_t)] \times 10^{-27}\ e\cdot\mathrm{cm}. \quad (94)$$

As benchmark points, take $c_V = c_\pm = 0.5$, $|c_t| = 1$. For both CMS and ATLAS data, small $\alpha(< \pi/2)$ is favored. Take $\alpha_t' = 1.2$ around the best fit point; thus, $\alpha_t \approx 1.0$, and the EDM data strongly constrain the coupling c_e. For most $\alpha_e \equiv \arg(c_e)$, the coupling strength $|c_e|$ is constrained to be as small as $\mathcal{O}(10^{-2}$–$10^{-1})$. But for some special angles, as $\alpha_e \approx -2.04$ and $\alpha_e \approx 1.09$, $|c_e|$ may be as large as $\mathcal{O}(1)$. But the windows are very narrow; in Fig. 9 we show the constraints close to the special angles.

If adding the contributions from heavy neutral Higgs bosons, the constraints on c_e would be shifted. Since both heavy scalars are CP even dominant, we can estimate that

$$\arg(c_{e,2}) \simeq \arg(c_{e,3}) \simeq \arg(c_{t,2}) \simeq \arg(c_{t,3}) \sim \mathcal{O}(0.1), \quad (95)$$

and for the two $|c_{e,i}|$, at least one of them is of $\mathcal{O}(1)$ because of its mass, which is the same for $|c_{t,i}|$. For the couplings to gauge bosons, we can estimate

$$c_2^2 + c_3^2 = 1 - c_1^2 \simeq 0.7; \quad (96)$$

thus, at least one of them must be large enough to be close to $\mathcal{O}(1)$. For a neutral Higgs boson with mass $m_2 \sim 300$ GeV or $m_2 \sim 700$ GeV, the contributions can be estimated as

$$d_{e,2} \simeq (1\text{–}5) \times 10^{-28}\ e\,\mathrm{cm}; \quad (97)$$

$$d_{e,3} \simeq (0.5\text{–}3) \times 10^{-28}\ e\,\mathrm{cm}. \quad (98)$$

As an example, if the heavy scalars contribute a $d_e' = 2 \times 10^{-28}\ e\,\mathrm{cm}$, Fig. 9 would be changed to Fig. 10. It still imposes strict constraints on c_e, but the behaviors are different from that without including the contributions from the heavy scalars.

For neutrons, the effective interaction can be written as [66,70,71]

$$\mathcal{L}_{n,\mathrm{EDM}} = -\frac{i}{2}\sum_q (d_q \bar{q}\sigma^{\mu\nu}\gamma^5 q F_{\mu\nu} + \tilde{d}_q g_s \bar{q}\sigma^{\mu\nu}\gamma^5 t^a q G^a_{\mu\nu}) - \frac{w}{3} f^{abc} G_{\mu\nu} G^{\nu,b}_{\sigma} \tilde{G}^{\mu\sigma,c} + \frac{\theta\alpha_s}{8\pi} G_{\mu\nu}\tilde{G}^{\mu\nu}. \quad (99)$$

The first two operators correspond to the EDM(d_q) and color EDM($\tilde{d}_q$)(CEDM) of light quarks; the third operator is the Weinberg operator; and the last operator, in which $\theta = \arg(\det(M_u \cdot M_d))$, is the strong *CP* phase. The EDM of the neutron [66,70,71] is

$$\frac{d_n}{e} \simeq 1.4\left(\frac{d_d}{e} - 0.25\frac{d_u}{e}\right) + 1.1(\tilde{d}_d + 0.5\tilde{d}_u) + (2.5\times 10^{-16}\theta + 4.3\times 10^{-16} w(\mathrm{GeV}^{-2}))\,\mathrm{cm} \quad (100)$$

at the hadron scale with a theoretical uncertainty of about 50%. At weak scale the EDM and CEDM for quarks are given as [70,71]

$$\frac{d_q}{e} = \frac{2\sqrt{2}\alpha_{em} Q_q G_F m_q}{(4\pi)^3}\left(c_V \mathrm{Im}(c_q) J_1(m_W, m_h) + c_\pm \mathrm{Im}(c_q) J_0(m_{H^\pm}, m_h) - \frac{8}{3}(\mathrm{Re}(c_q)\mathrm{Im}(c_t) J_{1/2}(m_t, m_h) + \mathrm{Im}(c_q)\mathrm{Re}(c_t) J'_{1/2}(m_t, m_h))\right); \quad (101)$$

$$\tilde{d}_q = -\frac{2\sqrt{2}\alpha_s G_F m_q}{(4\pi)^3}(\mathrm{Re}(c_q)\mathrm{Im}(c_t) J_{1/2}(m_t, m_h) + \mathrm{Im}(c_q)\mathrm{Re}(c_t) J'_{1/2}(m_t, m_h)); \quad (102)$$

and the Weinberg operator [70]

$$w = \frac{\sqrt{2} G_F g_s \alpha_s}{4\cdot(4\pi)^3}\mathrm{Re}(c_t)\mathrm{Im}(c_t) g\left(\frac{m_t^2}{m_h^2}\right) \quad (103)$$

with

$$g(x) = 4x^2 \int_0^1 dv \int_0^1 du \frac{u^3 v^3 (1-v)}{(xv(1-uv) + (1-u)(1-v))^2}. \quad (104)$$

Following the appendix in [70], with the input $m_u = 2.3$ MeV, $m_d = 4.8$ MeV and $\alpha_s(m_t) = 0.11$ [28], numerically, the EDM for the neutron is

$$\begin{aligned} d_n \simeq (0.5\text{–}1.5)\times(&-(7.0\mathrm{Re}(c_u)\mathrm{Im}(c_t) + 4.9\mathrm{Im}(c_u)\mathrm{Re}(c_t)) \\ &-(29\mathrm{Re}(c_d)\mathrm{Im}(c_t) + 20\mathrm{Im}(c_d)\mathrm{Re}(c_t)) \\ &-(2.8c_V + 0.25c_\pm)\mathrm{Im}(c_d) - (0.66c_V + 0.06c_\pm)\mathrm{Im}(c_u) \\ &+ 2.5\times 10^{10}\theta + 2.3|c_t|^2\sin(2\alpha'_t))\times 10^{-26}\, e\cdot\mathrm{cm}. \end{aligned} \quad (105)$$

Take benchmark points as usual, and fix $c_V = c_\pm = 0.5$ and $|c_t| = 1$, $\alpha_t = 1.0$ as usual. For $|c_u| \simeq |c_d| \sim \mathcal{O}(0.1)$, there are almost no constraints on $\alpha_u \equiv \arg(c_u)$ and $\alpha_d \equiv \arg(c_d)$. For $|c_u| \simeq |c_d| \sim \mathcal{O}(1)$, constraints on α_d and α_u are shown in Fig. 11. Ignoring the θ term, for $|c_u| = |c_d| = 1$, α_d is constrained in two bands with a width of $\Delta\alpha_d \simeq (0.2\text{–}1)$ from the uncertainties in calculating d_n. And the widths are more sensitive to c_d, for example, if $|c_d| = 0.5$, $\Delta\alpha_d \simeq (0.5\text{–}2)$. The constraints by neutron EDM are less strict compared with those by electron EDM in this model. Contributions from heavy neutral

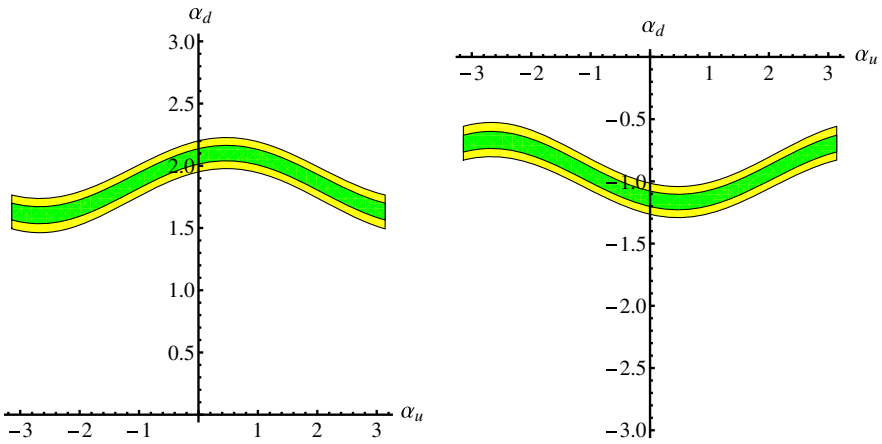

FIG. 11 (color online). Plots on the allowed $\alpha_d - \alpha_u$, taking $\alpha_t = 1.0$.

Higgs bosons and nonzero $\theta(\lesssim 10^{-10})$ would also change the location of the bands.

B. Meson mixing and *CP* violation

In the SM the neutral mesons K^0, D^0, B_d^0, and B_s^0 mix with their corresponding antiparticles through weak interactions. Usually, BSM will give additional contributions to the mixing matrix elements $\langle \bar{M}^0|\mathcal{H}_{\Delta F=2}|M^0\rangle$; thus, they will modify the mass splitting and mixing induced *CP*-violation observables. We can parametrize the new physics effects as [72]

$$M_{12,M} \equiv \frac{1}{2m_M}\langle \bar{M}^0|\mathcal{H}_{\Delta F=2}|M^0\rangle = M_{12,M,\mathrm{SM}}(1+\Delta_M e^{i\delta_M}). \tag{106}$$

For mass splitting, we list the world averaging results [28,73,74] and SM predictions [75–77] for Δm in Table VII. The useful decay constants and bag parameters are from the lattice results [78]. Only for the $D^0-\bar{D}^0$ system it is difficult to predict Δm_D since the long-distance effects are the dominant contributions. Nonzero δ_M from new physics will modify the *CP*-violated effects from those in the SM; thus, it will be constrained by *CP*-violated observable, as ϵ_K in $K^0-\bar{K}^0$ mixing and $\sin(2\beta_{d(s)})$ in $B_{d(s)}^0-\bar{B}_{d(s)}^0$ mixing. They are defined as

$$\epsilon_K = \frac{1}{3}\left(\frac{\mathcal{M}(K_L\to 2\pi^0)}{\mathcal{M}(K_S\to 2\pi^0)}\right)+\frac{2}{3}\left(\frac{\mathcal{M}(K_L\to \pi^+\pi^-)}{\mathcal{M}(K_S\to \pi^+\pi^-)}\right), \tag{107}$$

where $K_{L(S)}$ is the long (short) lived neutral kaon and $\mathcal{M}$ is the amplitude for the process and

$$\beta = \arg\left(-\frac{V_{tb}V_{td}^*}{V_{cb}V_{cd}^*}\right), \qquad \beta_s = \arg\left(\frac{V_{tb}V_{ts}^*}{V_{cb}V_{cs}^*}\right), \tag{108}$$

where V_{ij} are CKM matrix elements.

First, assuming the charged Higgs boson is heavy and considering the contribution only from the 126 GeV Higgs boson, we can write the flavor-changing effective interaction as

$$\mathcal{L}_{ij} = \bar{f}_i(\xi_{1ij}+\xi_{2ij}\gamma^5)f_j h + \mathrm{H.c.} \tag{109}$$

TABLE VII. SM predictions and experimental values for mass difference in meson mixing.

Meson	Δm_{exp} (GeV)	Δm_{SM} (GeV)
$K^0(d\bar{s})$	$(3.474\pm 0.006)\times 10^{-15}$	$(3.30\pm 0.34)\times 10^{-15}$
$D^0(c\bar{u})$	$(1.0\pm 0.3)\times 10^{-14}$	$\cdots$
$B_d^0(d\bar{b})$	$(3.33\pm 0.03)\times 10^{-13}$	$(3.3\pm 0.4)\times 10^{-13}$
$B_s^0(s\bar{b})$	$(1.1663\pm 0.0015)\times 10^{-11}$	$(1.14\pm 0.17)\times 10^{-11}$

The lightest neutral Higgs boson contribution to matrix elements for meson mixing is [79,80]

$$M_{12,M,\mathrm{SM}}\Delta_M e^{i\delta_M} = \frac{f_M^2 B_M m_M}{6m_h^2}\left(\xi_{1ij}^2-\xi_{2ij}^2+\frac{(\xi_{1ij}^2-11\xi_{2ij}^2)m_M^2}{(m_i+m_j)^2}\right). \tag{110}$$

The parameters f_M, B_M, and m_M are the decay constant, bag parameter, and mass for meson M^0, and $m_{i(j)}$ are masses for the quark $f_{i(j)}$. For $B_{d(s)}^0-\bar{B}_{d(s)}^0$ mixing, according to fitting results [81] (see the plots in [82] for details), for different $\delta_{B_d(B_s)}$,

$$\Delta_{B_d}\lesssim (0.1\text{–}0.4) \quad \text{and} \quad \Delta_{B_s}\lesssim (0.1\text{–}0.3). \tag{111}$$

For $\delta_{B_d(B_s)}=0$, the upper limit on $\Delta_{B_d(B_s)}$ is about 0.2. Comparing with (106) and (110) and adopting the Cheng-Sher ansatz [43], the typical upper limit on $\xi_{bs(bd)}$ has the order

$$\frac{|\xi_{bs}|v}{\sqrt{2m_b m_s}}\lesssim 2\times 10^{-2} \quad \text{and} \quad \frac{|\xi_{bd}|v}{\sqrt{2m_b m_d}}\lesssim 6\times 10^{-2}, \tag{112}$$

both of $\mathcal{O}(10^{-2}\text{–}10^{-1})$. For $D^0-\bar{D}^0$ mixing, we have the upper limit

$$\frac{|\xi_{cu}|v}{\sqrt{2m_c m_u}}\lesssim 0.1. \tag{113}$$

For $K^0-\bar{K}^0$ mixing, when $\delta_K\approx 0$ or π, we have $\Delta_K\lesssim 0.25$, which leads to

$$\frac{|\xi_{sd}|v}{\sqrt{2m_s m_d}}\lesssim 2\times 10^{-2}, \tag{114}$$

while for a general δ_K, Δ_K is strongly constrained to be less than $\mathcal{O}(10^{-3})$ because of the smallness of ϵ_K. New *CP*-violation effects must be very small in neutral K system while they are allowed or even favored [81] for other mesons.

Next, consider the contribution to $B_{d(s)}^0-\bar{B}_{d(s)}^0$ mixing from charged Higgs boson. Box diagrams with one or two charged Higgs boson instead of W boson will contribute to $\Delta_{B_d(B_s)}\exp(i\delta_{B_d(B_s)})$ as [83,84]

$$\Delta_{B_d(B_s)}e^{i\delta_{B_d(B_s)}} = \frac{\mathcal{F}_1(x_{tW},x_{tH},x_{HW})+\mathcal{F}_2(x_{tH})}{\mathcal{F}_0(x_{tW})}, \tag{115}$$

where

$$\mathcal{F}_0(x_{tW}) = 1 + \frac{9}{1-x_{tW}} - \frac{6}{(1-x_{tW})^2} - \frac{6x_{tW}^2 \ln x_{tW}}{(1-x_{tW})^3} \tag{116}$$

$$\mathcal{F}_1(x_{tW}, x_{tH}, x_{HW}) = \eta_{d(s)}^2 \frac{x_{tH}}{1-x_{HW}} \left(\frac{8-2x_{tW}}{1-x_{tH}} + \frac{(2x_{HW}-8)\ln x_{tH}}{(1-x_{tH})^2} + \frac{6x_{HW}\ln x_{tW}}{(1-x_{tW})^2} \right) \tag{117}$$

$$\mathcal{F}_2(x_{tH}) = \eta_{d(s)}^4 x_{tH} \frac{1 - x_{tH}^2 + 2x_{tH}\ln x_{tH}}{(1-x_{tH})^3} \tag{118}$$

at leading order in which $\eta_{d(s)} \approx (\xi_{1tb}\xi_{1td(s)}/2V_{tb}V_{ts(d)}^*)^{1/2}$ v/m_t and $x_{ij} = (m_i/m_j)^2$. We can parametrize the interactions (80) as

$$\mathcal{L}_{I,tD_iH^+} = -\frac{V_{tD_i}}{v}\bar{t}(X_t m_t P_L + X_{D_i} m_{D_i} P_R) D_i + \text{H.c.}, \tag{119}$$

in which $P_{L(R)} = (1 \mp \gamma^5)/2$. Thus, $\eta_{d(s)} \approx |X_t| v/(\sqrt{2}m_t)$ and it is not sensitive to X_{D_i} if they are of the same order as X_t. According to the constraints in Sec. III E for light charged Higgs $m_{H^\pm} < m_t$, with a typical coupling $|X_t| \lesssim 0.5$, $\Delta_{B_d(B_s)} \lesssim 0.2$ holds for $m_{H^\pm} \geq 100$ GeV and additional *CP*-violation effects induced by charged Higgs boson mediated loop are negligible. Thus, take a benchmark point $m_{H^\pm} = 150$ GeV as usual; it is allowed by B-meson mixing data, while for heavy charged Higgs $m_{H^\pm} > m_t$, the coupling X_t is not constrained by $t \to bH^+$ decay process. We can give an upper limit $|X_t| \lesssim (0.6\text{–}1)$ when 200 GeV $< m_{H^\pm} <$ 600 GeV.

In the $D^0 - \bar{D}^0$ mixing, another useful constraint comes from the neutral Higgs boson mediated box diagram. Its contribution to Δm_D is [85]

$$\Delta m_D^* = \frac{G_F^2 v^4 |\xi_{tu}\xi_{tc}|^2}{12\pi^2 m_t^2} f_D^2 m_D B_B r \mathcal{F}_2(x_{th}) \approx 4 \times 10^{-9} |\xi_{tu}\xi_{tc}|^2 \tag{120}$$

where $r = (\alpha_s(m_t)/\alpha_s(m_b))^{6/23}(\alpha_s(m_b)/\alpha_s(m_c))^{6/25} \approx 0.8$ and loop function $\mathcal{F}_2$ is the same as that in (118). For Δm_D^* contributing less than the order of measured Δm_D, we have $|\xi_{tu}\xi_{tc}| \lesssim 1.5 \times 10^{-3}$ and hence we can put a stronger constraint than (83) on the flavor-changing interactions including top as

$$\frac{|\xi_{tu}\xi_{tc}| v^2}{2m_t\sqrt{m_u m_c}} \lesssim 5, \tag{121}$$

which is of $\mathcal{O}(1)$.

C. The *B* leptonic decays

The rare decay process $B_{s,d} \to \mu^+\mu^-$ has been measured by LHCb [86] and CMS [87] Collaborations, respectively, with the results

$$\overline{\text{Br}}(B_s \to \mu^+\mu^-) = \begin{cases} 2.9^{+1.1}_{-1.0} \times 10^{-9}, & (\text{LHCb}, 4.0\,\sigma \text{ significance}), \\ 3.0^{+1.0}_{-0.9} \times 10^{-9}, & (\text{CMS}, 4.3\,\sigma \text{ significance}) \end{cases}; \tag{122}$$

and

$$\overline{\text{Br}}(B_d \to \mu^+\mu^-) = \begin{cases} 3.7^{+2.5}_{-2.1} \times 10^{-10}, & (\text{LHCb}), \\ 3.5^{+2.5}_{-1.8} \times 10^{-10}, & (\text{CMS}) \end{cases}. \tag{123}$$

A combination result is $\overline{\text{Br}}(B_s \to \mu^+\mu^-) = (2.9 \pm 0.7) \times 10^{-9}$ by CMS and LHCb Collaborations [88]. There is no evidence for the process $B_d \to \mu^+\mu^-$. The results correspond to the SM prediction [89] (and updated results [90] in 2014),

$$\overline{\text{Br}}(B_s \to \mu^+\mu^-)_{\text{SM}} = (3.65 \pm 0.23) \times 10^{-9}, \tag{124}$$

$$\overline{\text{Br}}(B_d \to \mu^+\mu^-)_{\text{SM}} = (1.06 \pm 0.09) \times 10^{-10}, \tag{125}$$

where the modified branching ratio $\overline{\text{Br}}$ means the averaged time-integrated branching ratio and it has the relation with the branching ratio Br as [91,92]

$$\text{Br}(B_s \to \mu^+\mu^-) = \overline{\text{Br}}(B_s \to \mu^+\mu^-)\left(1 + \mathcal{O}\left(\frac{\Delta\Gamma}{\Gamma}\right)\right). \tag{126}$$

See Sec. D for details.

Consider the neutral Higgs boson mediated flavor-changing process first. Using the constraints in (112), we can estimate the contributions to $\text{Br}(B_{s(d)} \to \mu^+\mu^-)$ as

$$\delta\text{Br}(B_s \to \mu^+\mu^-) = \frac{m_{B_s}|c_\mu|^2}{8\pi\Gamma_{B_s,\text{tot}}}\left(\frac{f_{B_s} m_{B_s}^2 m_\mu}{(m_b + m_s) v m_h^2}\right)^2 \lesssim 4 \times 10^{-12}|c_\mu|^2; \tag{127}$$

$$\delta\text{Br}(B_d \to \mu^+\mu^-) = \frac{m_{B_d}|c_\mu|^2}{8\pi\Gamma_{B_d,\text{tot}}}\left(\frac{f_{B_d} m_{B_d}^2 m_\mu}{(m_b + m_d) v m_h^2}\right)^2 \lesssim 1 \times 10^{-12}|c_\mu|^2. \tag{128}$$

We cannot get stronger constraints through these processes on $|c_\mu|$ than direct search [93], which gives $|c_\mu| \lesssim 7$.

Next, consider the charged Higgs boson contribution. For $|X_t| \sim |X_{b,s,\mu}| \sim \mathcal{O}(1)$, the charged Higgs boson loop is sensitive to X_t and $m_{H^\pm}$ only [94]. According to [94], it is estimated that

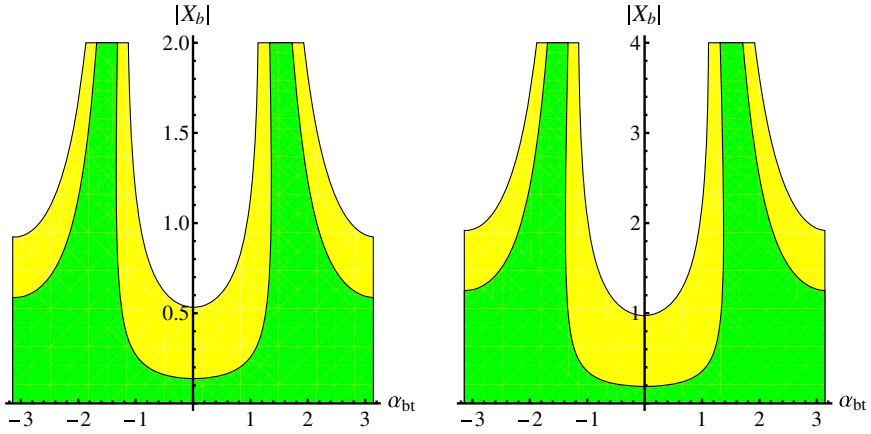

FIG. 12 (color online). Plots on allowed $\alpha_{bt} - |X_b|$. For the left figure, $|X_t| = 0.5$ and $m_{H^\pm} = 150$ GeV; for the right figure, $|X_t| = 0.8$ and $m_{H^\pm} = 500$ GeV.

$$\frac{\delta \mathrm{Br}(B_s \to \mu^+\mu^-)}{\mathrm{Br}(B_s \to \mu^+\mu^-)} \approx \left(1 - \frac{|X_t^2|}{\eta}\frac{Y_{\mathrm{2HDM}}}{Y_{\mathrm{SM}}}\right)^2, \tag{129}$$

where $\eta = 0.987$ is the electroweak and QCD correction factor and

$$Y_{\mathrm{SM}} = \frac{x_{tW}}{8}\left(\frac{x_{tW}-4}{x_{tW}-1} + \frac{3x_{tW}}{(x_{tW}-1)^2}\ln x_{tW}\right); \tag{130}$$

$$Y_{\mathrm{2HDM}} = \frac{x_{tW}^2}{8}\left(\frac{1}{x_{HW}-x_{tW}} + \frac{x_{HW}}{(x_{HW}-x_{tW})^2}\ln\left(\frac{x_{tW}}{x_{HW}}\right)\right). \tag{131}$$

If the charged Higgs boson is light, $(m_{H^\pm}) < m_t$, $|X_t| = 0.5$ is allowed at 95% C.L., while for a heavy charged Higgs boson, when 200 GeV $< m_{H^\pm} <$ 600 GeV, we have the 95% C.L. upper limit on $|X_t|$ as $|X_t| \lesssim (0.6\text{–}1.1)$ with the combined experimental results or $|X_t| \lesssim (0.8\text{–}1.4)$ with single experimental result.

D. The B radiative decays

The inclusive radiative decays branching ratio of $\bar{B}$ meson $\bar{B} \to X_s\gamma$ (or we say $b \to s\gamma$ at parton level) has the averaged value [73]

$$\mathrm{Br}(\bar{B} \to X_s\gamma) = (3.43 \pm 0.22) \times 10^{-4}, \tag{132}$$

with the photon energy $E_\gamma > 1.6$ GeV. The SM prediction for that value is $(3.15 \pm 0.23) \times 10^{-4}$ to $\mathcal{O}(\alpha_s^2)$ [56,95]. In a 2HDM, the dominant contribution to modify this decay rate is from a loop containing a charged Higgs boson instead of the W boson in the SM. The neutral Higgs loop contribution is negligible because of the suppression in ξ_{bs} and $m_{b(s)}/v$.

The charged Higgs boson loop is sensitive to both X_t and X_b thus we should take some benchmark points. Defining $\alpha_{bt} \equiv \arg(X_b/X_t)$, for a light charged Higgs boson, take $|X_t| = 0.5$ and $m_{H^\pm} = 150$ GeV as before; while for a heavy charged Higgs boson, take $|X_t| = 0.8$ and $m_{H^\pm} = 500$ GeV. We show the allowed region for $\alpha_{bt} - |X_b|$ in Fig. 12 utilizing the calculations in [56,96]. From the figures, we can see that for most α_{bt} the coupling $|X_b|$ is constrained to be $\lesssim \mathcal{O}(1)$; while for some angles it can be larger.[9]

V. FEATURES OF THE LEE MODEL AND ITS FUTURE PERSPECTIVES

One of the main goals of this paper is the phenomenological study of the Lee model with spontaneous CP violation [26]. We can see from the last two sections that the Lee model is still viable to confront the high and low energy experiments. The next natural question is how to confirm/exclude this model at future facilities.

In the scalar sector there are nine free parameters μ_1^2, μ_2^2, and $\lambda_{1,2,\ldots,7}$, corresponding to nine observables:

(i) Four masses m_h, m_2, m_3, and $m_{H^\pm}$;
(ii) VEVs and a physical phase v_1, v_2, ξ (or equivalently v, $\tan\beta$, ξ);
(iii) Two neutral scalar mixing angles; equivalently we choose the ratios c_1 and c_2 of the couplings to gauge boson compared to the corresponding ones in the SM.

We treat the discovered scalar with mass 126 GeV as the lightest neutral Higgs boson. If the Lee model is true, the extra neutral and charged Higgs bosons should be discovered at high energy colliders. As a general rule, the lighter the extra Higgs bosons, the easier they can be produced. In order to confirm the Lee model, another possible signal can be the FCNC decay of the neutral Higgs bosons that

[9]That is because with merely the decay rate, we can only determine the absolute value for the $b \to s\gamma$ amplitude. The largest allowed X_b can reach 14 for the left figure and 28 for the right figure, in which case the new physics contribution is twice as large as the SM but with the opposite sign.

are unobservably small in the SM. Furthermore, the *CP* properties of the Higgs boson are essential measurements, though measuring is a very challenging task.

As we have pointed out there is no SM limit in this scenario; thus, it is always testable at the future colliders, such as the LHC with $\sqrt{s} = 14$ TeV, CEPC, ILC, or TLEP with $\sqrt{s} = (240\text{–}250)$ TeV, even before the discovery of other neutral Higgs bosons and charged Higgs boson. The coupling between the lightest Higgs boson and other particles (especially for massive gauge bosons $W^{\pm}$ and Z^0) is usually suppressed by the factor of $\mathcal{O}(t_\beta s_\xi)$. In the $b\bar{b}$ decay channel or any VBF, V + H production channel, a significant suppression can be the first sign of this scenario. On the contrary if the signals become even more SM-like, this scenario will be disfavored.

For future LHC with $\sqrt{s} = 14$ TeV, the signal strengths will be measured with an uncertainty of about 10% at the luminosity 300 fb^{-1} [97,98]. Perform the same χ^2 fit as in (70), and add the $b\bar{b}$ decay mode in. The value of χ^2 is sensitive to c_V and c_b, and the magnitude of c_V is a criterion for this model. A Higgs boson with $c_V \gtrsim (0.6\text{–}0.7)$ is hardly pseudoscalar dominant; thus, if $c_V \lesssim (0.6\text{–}0.7)$ is excluded, we can say this scenario is excluded. So we can test this scenario by fitting the signal strengths. We list the estimating results in Table VIII.

If all signal strengths and the overall χ^2 are consist with SM at 1σ level, for the integrated luminosity 300 fb^{-1}, all $c_V \lesssim 0.62$ can be excluded at 95% C.L. (2σ) while all $c_V \lesssim 0.55$ can be excluded at 99.7% C.L. (3σ); For the integrated luminosity 3000 fb^{-1}, all $c_V \lesssim 0.77$ can be excluded at 95% C.L. (2σ) while all $c_V \lesssim 0.72$ can be excluded at 99.7% C.L. (3σ). If all signal strengths and the overall χ^2 are consistent with SM at 2σ level, for the integrated luminosity 300 fb^{-1}, all $c_V \lesssim 0.53$ can be excluded at 95% C.L. (2σ) while all $c_V \lesssim 0.45$ can be excluded at 99.7% C.L. (3σ); For the integrated luminosity 3000 fb^{-1}, all $c_V \lesssim 0.7$ can be excluded at 95% C.L. (2σ) while all $c_V \lesssim 0.65$ can be excluded at 99.7% C.L. (3σ). All the results are for the largest parameter space in this scenario because the true ability to test this scenario by χ^2 depends strongly on the real signal strengths from future experiments.

TABLE VIII. Abilities to test the scenario at $\sqrt{s} = 14$ TeV LHC. Lower limits for the allowed c_V at 2σ and 3σ levels are listed in the tables. For the top/bottom tables we assume that all signal strengths are consist with SM at 1 and 2σ level, respectively.

Excluded level	2σ	3σ
300 fb^{-1}	0.62	0.55
3000 fb^{-1}	0.77	0.72

Excluded level	2σ	3σ
300 fb^{-1}	0.53	0.45
3000 fb^{-1}	0.7	0.65

Another useful observable is f_{a3} defined in (2). For $\sqrt{s} = 14$ TeV, the 95% C.L. upper limit on f_{a3} will reach about 0.14 (0.04) for the luminosity 300(3000) fb^{-1} [97,98],[10] which leads to the constraints $|a_3/a_1| < 1.0(0.5) \sim \mathcal{O}(1)$ separately. For $|c_t| \sim \mathcal{O}(1)$, it is still too large to give direct constraints on $\alpha_t \equiv \arg(c_t)$.

At a Higgs boson factory with the e^+e^- initial state at $\sqrt{s} = (240\text{–}250)$ GeV, the dominant production process for a Higgs boson is associated with a Z^0 boson. Another important production process is through VBF. In this scenario it is suppressed by a factor c_1^2; thus, we can exclude this scenario if the total cross section favors the SM. For the total cross section, a measurement with $\mathcal{O}(10\%)$ uncertainty is accurate enough to distinguish the scenario we discussed in this paper and SM at 3σ or even 5σ significance. Such accuracy can be achieved at CEPC/ILC/TLEP. At $\sqrt{s} = 240$ GeV TLEP, the total cross section can be measured with an uncertainty 0.4% for the integrated luminosity 500 fb^{-1} [99,100], while that value is about 3% for the integrated luminosity 250 fb^{-1} ILC at $\sqrt{s} = 500$ GeV [101].

VI. CONCLUSIONS AND DISCUSSIONS

In this paper we proposed a scenario in which the smallness of *CP* violation and the lightness of the Higgs boson are correlated through small $t_\beta s_\xi$, based on the Lee model, namely, the 2HDM with spontaneous *CP* violation. The basic assumption is that *CP*, which is spontaneously broken by the complex vacuum, is an approximate symmetry. We found that m_h as well as the quantities K and J are $\propto t_\beta s_\xi$ in the limit $t_\beta s_\xi \to 0$. Here, K and J are the measures for *CP*-violation effects in scalar and Yukawa sectors, respectively. It is a new way to understand why the Higgs boson discovered at the LHC is light. In this scenario, all the three neutral physical degrees of freedom mix with each other; thus, none of them is a *CP* eigenstate.

We then investigated the phenomenological constraints from both high energy and low energy experiments and found the scenario still alive. The lightest Higgs boson usually couples with SM gauge and fermion particles with a smaller strength than in the SM; thus, the total width must be narrower than that in the SM. Such choice of the parameters makes the Lee model still allowed by the CMS or ATLAS data. The LHC search for heavy neutral bosons implies that the masses of the other two neutral bosons should be away from the region 300–700 GeV. The S-T

[10]Almost the same for the CMS and ATLAS detector, with 300(3000) fb^{-1} luminosity, the upper limit can reach 0.15 (0.037) for ATLAS and 0.13 (0.04) for CMS; see details in the references.

ellipse also strictly constrains the mass relation between the charged and neutral bosons as can be seen in Figs. 1–3. We also fitted the CMS and ATLAS data, respectively, for example, see Figs. 4–8. We found that this scenario is still allowed for either collaboration's data. It is not sensitive to the charged Higgs contribution. After considering all the data, a light charged Higgs boson with the mass of about 100 GeV is still allowed. Small $h\bar{b}b$ vertex is favored for both CMS and ATLAS data. The minimal χ^2 is close to the χ^2 in the SM; thus, we cannot conclude that the SM is better than the Lee model.

We forbid the explicit CP violation in the whole Lagrangian, including the Yukawa sector; thus, we must tolerate the tree-level FCNC. The flavor-changed couplings including top quark are constrained by the same sign top production process and the top quark rare decay, besides the constraints by B physics processes. The tree-level FCNC vertices including five light quarks are strongly constrained to be less than $\mathcal{O}(10^{-2}$–$10^{-1})\sqrt{2m_i m_j}/v$ while for the vertices including top quark it should be less than $\mathcal{O}(1)\sqrt{2m_t m_q}/v$. The coupling X_t for tbH^+ vertex is constrained to be less than $\mathcal{O}(0.1$–$1)$ for different $m_{H^\pm}$, while $X_b \sim \mathcal{O}(1)$ are usually allowed by $b \to s\gamma$ data.

The constraints by EDMs are usually very important in discussing a model with CP violation, because new sources of CP violation may modify the theoretical prediction of EDMs from the SM by several orders of magnitude, and may be testable by the experiments now. The EDM for electrons gave very strict constraints on the $h\bar{e}e$ vertex as shown in Figs. 9–10, while the EDMs for neutrons gave weaker constraints on $h\bar{d}d$ and $h\bar{u}u$ vertices; see Fig. 11.

There is no SM limit for the lightest Higgs boson in this scenario; thus, it is testable at future colliders. At $\sqrt{s} = 14$ TeV, besides discovering the extra neutral and charged Higgs bosons, the ability to test this scenario depends on how far the signal strengths for the 126 GeV Higgs boson differ from the SM predictions, as listed in Table VII. From the discovery point of view, if any suppression in the VBF, VH production channel or $b\bar{b}$ decay channel is confirmed, this scenario would be favored. On the contrary, if all signals are SM-like more and more at future colliders, this scenario would be disfavored by data. For most cases 300 fb^{-1} luminosity is not enough to exclude this scenario, while 3000 fb^{-1} luminosity is better. At $\sqrt{s} = (240$–$250)$ GeV e^+e^- colliders, several fb^{-1} luminosity is enough to distinguish this scenario and SM at $(3$–$5)\sigma$ level by accurately measuring the total cross section. We emphasize that measuring the CP properties and the flavor-changing decay of the Higgs bosons is essential to pin down the Lee model.

We did not build the model for the flavor sector in detail; thus, we did not solve the natural FCNC and strong CP problems. It is possible to solve the FCNC and strong CP problems together, for example, see the model proposed by Liao [102]. We also did not discuss the constraints from flavor-changing processes in the lepton sector. As a model with CP violation, there may also be some new CP-violation effects, especially in top, τ, and neutral D sector where no CP violation has been discovered. We did not study the cosmological effects in this paper, like the domain wall and electroweak baryogenesis in this model. All these consequences will be further scrutinized in the future.

ACKNOWLEDGMENTS

We thank J.-J. Cao, Q.-H. Cao, S.-L. Chen, L. Dai, W. Liao, C. Zhang, *et al.* for helpful discussion. This work was supported in part by the Natural Science Foundation of China (Grants No. 11135003 and No. 11375014).

APPENDIX A: VACUUM STABILITY CONDITIONS

For the potential (10), when $|\phi_i| \equiv \sqrt{\phi_i^\dagger \phi_i} \to \infty$, $V \geq 0$ must hold to keep the vacuum stable. Writing $|\phi_1| = r_1$, $|\phi_2| = r_2$, and $\phi_1^\dagger \phi_2 = r\exp(i\alpha)$, we have

$$|\phi_1^\dagger \phi_2| = r \leq |\phi_1| \cdot |\phi_2| = r_1 r_2. \tag{A1}$$

The R_{ij} and I_{ij} can be expressed as

$$\begin{aligned} &R_{11} = r_1^2, \qquad R_{22} = r_2^2, \qquad R_{12} = r\cos\alpha, \\ &I_{12} = r\sin\alpha. \end{aligned} \tag{A2}$$

Thus, we have that the equation

$$\begin{aligned} V = {} & \lambda_1 r_1^4 + \lambda_3 r_1^2 r_2^2 + \lambda_6 r_2^4 \\ & + r c_\alpha (\lambda_2 r_1^2 + \lambda_5 r_2^2) + r^2 (\lambda_4 c_\alpha^2 + \lambda_7 s_\alpha^2) \end{aligned} \tag{A3}$$

holds for any α and $0 \leq r \leq r_1 r_2$.

Another type of condition is that the potential should be minimized when

$$\langle \phi_1 \rangle = \frac{1}{\sqrt{2}} \begin{pmatrix} 0 \\ v_1 \end{pmatrix}, \qquad \langle \phi_2 \rangle = \frac{1}{\sqrt{2}} \begin{pmatrix} 0 \\ v_2 e^{i\xi} \end{pmatrix}. \tag{A4}$$

It is equivalent to the conditions that the mass matrix for neutral Higgs boson, $\tilde{m}$ in (19), must be positive definite. We write the conditions as

$$\mathrm{tr}\tilde{m} > 0, \qquad (\mathrm{tr}\tilde{m})^2 - \mathrm{tr}(\tilde{m})^2 > 0, \qquad \det \tilde{m} > 0. \tag{A5}$$

If there exists more than one local minimal point for the potential, the physical vacuum should be chosen at the global minimum if we want to forbid a metastable vacuum.

APPENDIX B: SCALAR SPECTRA AND SMALL $t_\beta s_\xi$ EXPANSION

In the unitary gauge the mass square matrix for charged scalars reads

$$M_{\pm}^2 = -\frac{\lambda_7}{2}\begin{pmatrix} v_2^2 & -v_1 v_2 e^{-i\xi} \\ -v_1 v_2 e^{i\xi} & v_1^2 \end{pmatrix}. \quad \text{(B1)}$$

The eigenvalues are

$$m_{G^\pm}^2 = 0; \qquad m_{H^\pm}^2 = -\frac{\lambda_7 v^2}{2}; \quad \text{(B2)}$$

where the zero eigenvalue corresponds to the charged goldstones, which will be eaten by the longitudinal part of W bosons. Diagonalize (B1) by performing a rotation,

$$\begin{pmatrix} G^+ \\ H^+ \end{pmatrix} = \begin{pmatrix} \cos\beta & e^{-i\xi}\sin\beta \\ -e^{i\xi}\sin\beta & \cos\beta \end{pmatrix}\begin{pmatrix} \phi_1^+ \\ \phi_2^+ \end{pmatrix}. \quad \text{(B3)}$$

For the neutral parts, in the basis $(I_1, I_2, R_1, R_2)^T$, for any angle α to appear below, we have the mass square matrix $M_0^2 = (v^2/2)m_{ij}$, where

$$\begin{aligned}
m_{11} &= (\lambda_4 - \lambda_7)s_\beta^2 s_\xi^2; \\
m_{12} &= \lambda_5 s_\beta^2 s_\xi^2; \\
m_{13} &= (\lambda_2 c_\beta + (\lambda_4 - \lambda_7)s_\beta c_\xi)s_\beta s_\xi; \\
m_{14} &= ((\lambda_4 - \lambda_7)c_\beta + \lambda_5 s_\beta c_\xi)s_\beta s_\xi; \\
m_{22} &= 4\lambda_6 s_\beta^2 s_\xi^2; \\
m_{23} &= 2((\lambda_3 + \lambda_7)c_\beta + \lambda_5 s_\beta c_\xi)s_\beta s_\xi; \\
m_{24} &= (\lambda_5 c_\beta + 4\lambda_6 s_\beta c_\xi)s_\beta s_\xi; \\
m_{33} &= 4\lambda_1 c_\beta^2 + 2\lambda_2 c_\beta s_\beta c_\xi + (\lambda_4 - \lambda_7)c_\xi^2 s_\beta^2; \\
m_{34} &= \lambda_2 c_\beta^2 + (2\lambda_3 + \lambda_4 + \lambda_7)s_\beta c_\beta c_\xi + \lambda_5 s_\beta^2 c_\xi^2; \\
m_{44} &= (\lambda_4 - \lambda_7)c_\beta^2 + 2\lambda_5 c_\beta s_\beta c_\xi + 4\lambda_6 s_\beta^2 c_\xi^2.
\end{aligned}$$

Perform the same rotation as (B3) between ϕ_1 and ϕ_2, which in the basis above can be written as

$$R = R_1 R_2 = \begin{pmatrix} c_\beta & s_\beta & 0 & 0 \\ -s_\beta & c_\beta & 0 & 0 \\ 0 & 0 & 1 & 0 \\ 0 & 0 & 0 & 1 \end{pmatrix}\begin{pmatrix} 1 & 0 & 0 & 0 \\ 0 & c_\xi & 0 & -s_\xi \\ 0 & 0 & 1 & 0 \\ 0 & s_\xi & 0 & c_\xi \end{pmatrix}, \quad \text{(B4)}$$

and we have

$$\tilde{M}_0^2 = R M_0^2 R^{-1} = \frac{v^2}{2}\begin{pmatrix} 0 & \\ & (\tilde{m})_{3\times 3} \end{pmatrix}, \quad \text{(B5)}$$

where the zero eigenvalue corresponds to the neutral Goldstone,

$$G^0 = c_\beta I_1 + s_\beta c_\xi I_2 - s_\beta s_\xi R_2, \quad \text{(B6)}$$

which will be eaten by the longitudinal part of Z boson. The matrix elements for $\tilde{m}$ in the basis $(-s_\beta I_1 + c_\beta c_\xi I_2 - c_\beta s_\xi R_2, R_1, s_\xi I_2 + c_\xi R_2)^T$ should be

$$\begin{aligned}
\tilde{m}_{11} &= (\lambda_4 - \lambda_7)s_\xi^2; \\
\tilde{m}_{12} &= -(\lambda_2 c_\beta + (\lambda_4 - \lambda_7)s_\beta c_\xi)s_\xi; \\
\tilde{m}_{13} &= -(\lambda_5 s_\beta + (\lambda_4 - \lambda_7)c_\beta c_\xi)s_\xi; \\
\tilde{m}_{22} &= 4\lambda_1 c_\beta^2 + 2\lambda_2 c_\beta s_\beta c_\xi + (\lambda_4 - \lambda_7)s_\beta^2 c_\xi^2; \\
\tilde{m}_{23} &= \lambda_2 c_\beta^2 c_\xi + (2(\lambda_3 + \lambda_7) + (\lambda_4 - \lambda_7)c_\xi^2)s_\beta c_\beta + \lambda_5 s_\beta^2 c_\xi; \\
\tilde{m}_{33} &= (\lambda_4 - \lambda_7)c_\beta^2 c_\xi^2 + 2\lambda_5 s_\beta c_\beta c_\xi + 4\lambda_6 s_\beta^2. \quad \text{(B7)}
\end{aligned}$$

We can expand $\tilde{m}$ in powers of $t_\beta s_\xi$ as follows:

$$\tilde{m} = \tilde{m}_0 + (t_\beta s_\xi)\tilde{m}_1 + (t_\beta s_\xi)^2\tilde{m}_2 + \cdots \quad \text{(B8)}$$

In the basis $(-s_\beta I_1 + c_\beta c_\xi I_2 - c_\beta s_\xi R_2, R_1, s_\xi I_2 + c_\xi R_2)^T$ the matrix $\tilde{m}_0$ can be written as

$$\tilde{m}_0 = \begin{pmatrix} (\lambda_4 - \lambda_7)s_\xi^2 & -\lambda_2 s_\xi & -(\lambda_4 - \lambda_7)s_\xi c_\xi \\ -\lambda_2 s_\xi & 4\lambda_1 & \lambda_2 c_\xi \\ -(\lambda_4 - \lambda_7)s_\xi c_\xi & \lambda_2 c_\xi & (\lambda_4 - \lambda_7)c_\xi^2 \end{pmatrix}. \quad \text{(B9)}$$

Diagonalizing it with a 3×3 matrix,

$$r = r_1 r_2 = \begin{pmatrix} 1 & 0 & 0 \\ 0 & c_\theta & s_\theta \\ 0 & -s_\theta & c_\theta \end{pmatrix}\begin{pmatrix} c_\xi & 0 & s_\xi \\ 0 & 1 & 0 \\ -s_\xi & 0 & c_\xi \end{pmatrix}, \quad \text{(B10)}$$

we have

$$r\tilde{m}_0 r^{-1} = \begin{pmatrix} 0 & & \\ & (\tilde{m}_0)_{22} & \\ & & (\tilde{m}_0)_{33} \end{pmatrix}, \quad \text{(B11)}$$

in which

$$\begin{aligned}
(\tilde{m}_0)_{22(33)} &= \frac{4\lambda_1 + \lambda_4 - \lambda_7}{2} \\
&\quad \pm \left(\frac{4\lambda_1 - (\lambda_4 - \lambda_7)}{2}c_{2\theta} + \lambda_2 s_{2\theta}\right); \quad \text{(B12)}
\end{aligned}$$

$$\theta = \frac{1}{2}\arctan\left(\frac{2\lambda_2}{4\lambda_1 - (\lambda_4 - \lambda_7)}\right). \quad \text{(B13)}$$

The two heavy scalars have their masses

$$m_{2(3)}^2 = \frac{v^2}{2}((\tilde{m}_0)_{22(33)} + \mathcal{O}(t_\beta s_\xi)). \quad \text{(B14)}$$

The new basis is then

$$r\begin{pmatrix} c_\xi I_2 - s_\xi R_2 \\ R_1 \\ s_\xi I_2 + c_\xi R_2 \end{pmatrix} = \begin{pmatrix} I_2 \\ c_\theta R_1 + s_\theta R_2 \\ -s_\theta R_1 + c_\theta R_2 \end{pmatrix}, \tag{B15}$$

in which the useful matrix elements for $\tilde{m}$ are

$$(\tilde{m}_1)_{11} = 0; \tag{B16}$$

$$(\tilde{m}_1)_{12} = (2(\lambda_3+\lambda_7)c_\theta + \lambda_5 s_\theta); \tag{B17}$$

$$(\tilde{m}_1)_{13} = (\lambda_5 c_\theta - 2(\lambda_3+\lambda_7)s_\theta); \tag{B18}$$

$$(\tilde{m}_2)_{11} = 4\lambda_6. \tag{B19}$$

Thus, to the leading order of $t_\beta s_\xi$, for the lightest scalar h we have

$$\begin{aligned} m_h^2 &= \frac{v^2 t_\beta^2 s_\xi^2}{2}\left(\frac{(\tilde{m}_1)_{12}^2}{(\tilde{m}_0)_{22}} + \frac{(\tilde{m}_1)_{13}^2}{(\tilde{m}_0)_{33}} + (\tilde{m}_2)_{11}\right) \\ &= \frac{v^2 t_\beta^2 s_\xi^2}{2}\left[4(\lambda_3+\lambda_7)^2\left(\frac{c_\theta^2}{(\tilde{m}_0)_{22}} + \frac{s_\theta^2}{(\tilde{m}_0)_{33}}\right) + \lambda_5^2\left(\frac{s_\theta^2}{(\tilde{m}_0)_{22}} + \frac{c_\theta^2}{(\tilde{m}_0)_{33}}\right) - 2\lambda_5(\lambda_3+\lambda_7)s_{2\theta}\left(\frac{1}{(\tilde{m}_0)_{22}} - \frac{1}{(\tilde{m}_0)_{33}}\right) + 4\lambda_6\right]; \end{aligned} \tag{B20}$$

$$\begin{aligned} h &= I_2 + t_\beta s_\xi\left(\frac{(\tilde{m}_1)_{12}}{(\tilde{m}_0)_{22}}(c_\theta R_1 + s_\theta R_2) + \frac{(\tilde{m}_1)_{13}}{(\tilde{m}_0)_{33}}(c_\theta R_2 - s_\theta R_1) - \frac{I_1}{t_\xi}\right) \\ &= I_2 + t_\beta s_\xi\left[\left(2(\lambda_3+\lambda_7)\left(\frac{c_\theta^2}{(\tilde{m}_0)_{22}} + \frac{s_\theta^2}{(\tilde{m}_0)_{33}}\right) + \frac{\lambda_5 s_{2\theta}}{2}\left(\frac{1}{(\tilde{m}_0)_{22}} - \frac{1}{(\tilde{m}_0)_{33}}\right)\right)R_1 + \left((\lambda_3+\lambda_7)s_{2\theta}\left(\frac{1}{(\tilde{m}_0)_{22}} - \frac{1}{(\tilde{m}_0)_{33}}\right)\right. \right. \\ &\quad \left.\left. + \lambda_5\left(\frac{s_\theta^2}{(\tilde{m}_0)_{22}} + \frac{c_\theta^2}{(\tilde{m}_0)_{33}}\right)\right)R_2 - \frac{I_1}{t_\xi}\right]. \end{aligned} \tag{B21}$$

APPENDIX C: SOME USEFUL FEYNMAN RULES IN THIS MODEL

From the Lagrangian we have some useful coupling vertices directly,

$$\mathcal{L}_{hVV} = \left(\frac{2m_W^2}{v}W_\mu^+ W^{\mu-} + \frac{m_Z^2}{v}Z_\mu Z^\mu\right)(c_\beta R_1 + s_\beta c_\xi R_2 + s_\beta s_\xi I_2); \tag{C1}$$

$$\begin{aligned} \mathcal{L}_{hH^+H^-} = -vH^+H^-\left[\frac{\lambda_2+\lambda_5}{2}s_\beta s_\xi I_1 + \left(\lambda_3 c_\beta^2 + \left(-\lambda_2 + \frac{\lambda_5}{2}\right)c_\beta^2 s_\beta c_\xi + (2\lambda_1 - \lambda_4 c_\xi^2 - \lambda_7 s_\xi^2)c_\beta s_\beta^2 + \frac{\lambda_2}{2}s_\beta^3 c_\xi\right)R_1 \right. \\ \left. + ((2\lambda_6 - \lambda_7)c_\beta^2 - \lambda_5 c_\beta s_\beta c_\xi + \lambda_3 s_\beta^2)I_2 + \left(\frac{\lambda_5}{2}c_\beta^3 - (\lambda_4 - 2\lambda_6)c_\beta^2 s_\beta c_\xi + \left(\frac{\lambda_2}{2} - \lambda_5 c_\xi^2\right)c_\beta s_\beta^2 + \lambda_3 s_\beta^3 c_\xi\right)R_2\right]; \end{aligned} \tag{C2}$$

$$\mathcal{L}_{hDD} = -\frac{1}{\sqrt{2}}\bar{D}_{Li}(Y'_{1d}(R_1 + iI_1) + Y'_{2d}(R_2 + iI_2))_{ij}D_{Rj} + \text{H.c.}; \tag{C3}$$

$$\mathcal{L}_{hUU} = -\frac{1}{\sqrt{2}}\bar{U}_{Li}(Y'_{1u}(R_1 - iI_1) + Y'_{2u}(R_2 - iI_2))_{ij}U_{Rj} + \text{H.c.}; \tag{C4}$$

$$\mathcal{L}_{Ch} = -\frac{1}{\sqrt{2}}\bar{U}_{Li}(V_{\text{CKM}})_{ij}(-Y'_{1d}s_\beta e^{-i\xi} + Y'_{2d}c_\beta)_{jk}D_{Rk}H^+ - \frac{1}{\sqrt{2}}\bar{D}_{Li}(V_{\text{CKM}}^\dagger)_{ij}(Y'_{1u}s_\beta e^{i\xi} - Y'_{2u}c_\beta)_{ji}U_{Rk}H^- + \text{H.c.} \tag{C5}$$

The Y' in Yukawa couplings means the couplings in the mass eigenstates. For neutral Higgs triple vertex, the Feynman rules are all from

$$-i\lambda_{ijk} = -\frac{i\partial^3 V}{\partial h_i \partial h_j \partial h_k}. \tag{C6}$$

APPENDIX D: FORMALISM FOR NEUTRAL MESON

The mesons K^0, D^0, B_d^0, and B_s^0 can mix with their charged conjugate particles, through weak interaction in the SM. We begin with the Schrödinger equation

$$i\frac{\partial}{\partial t}\begin{pmatrix}|M_0\rangle\\ |\bar{M}_0\rangle\end{pmatrix} = \left(\mathbf{m} - \frac{i}{2}\Gamma\right)\begin{pmatrix}|M_0\rangle\\ |\bar{M}_0\rangle\end{pmatrix}, \tag{D1}$$

where $\mathbf{m}$ and $\mathbf{\Gamma}$ are a 2×2 matrix. Writing the Hamiltonian as

$$\mathcal{H} = \mathcal{H}_0 + \mathcal{H}_{\Delta F=1} + \mathcal{H}_{\Delta F=2}, \tag{D2}$$

we have the matrix elements

$$\left(\mathbf{m} - \frac{i}{2}\Gamma\right)_{ij} = m_M\delta_{ij} + \frac{1}{2m_M}\langle\psi_i|\mathcal{H}_{\Delta F=2}|\psi_j\rangle + \frac{1}{2m_M}\int d\Pi_f \frac{\langle\psi_i|\mathcal{H}_{\Delta F=1}|f\rangle\langle f|\mathcal{H}_{\Delta F=1}|\psi_j\rangle}{m_M - E(f) + i\epsilon} \tag{D3}$$

with the normalized condition $\langle\psi_i|\psi_j\rangle = 2m_M\delta_{ij}$ where $\psi_{i,j} = |M^0\rangle$ or $\bar{M}^0$. The second and third terms come from short-distance and long-distance effects separately and according to (D3)

$$\Gamma_{ij} = \frac{1}{2m_M}\int d\Pi_f \langle\psi_i|\mathcal{H}_{\Delta F=1}|f\rangle \times \langle f|\mathcal{H}_{\Delta F=1}|\psi_j\rangle 2\pi\delta(E(f) - m_M). \tag{D4}$$

The solutions for the eigenvalues are

$$m_{H(L)} = m_M \pm \mathrm{Re}\left(\sqrt{\left(\mathbf{m}_{12} - \frac{i}{2}\Gamma_{12}\right)\left(\mathbf{m}_{12}^* - \frac{i}{2}\Gamma_{12}^*\right)}\right); \tag{D5}$$

$$\Gamma_{H(L)} = \Gamma \mp \mathrm{Im}\left(\sqrt{\left(\mathbf{m}_{12} - \frac{i}{2}\Gamma_{12}\right)\left(\mathbf{m}_{12}^* - \frac{i}{2}\Gamma_{12}^*\right)}\right) \tag{D6}$$

The H(L) means the heavy (light) mass eigenstate

$$|M_{H(L)}\rangle = p|M^0\rangle \mp q|\bar{M}^0\rangle, \tag{D7}$$

where

$$|p|^2 + |q|^2 = 1; \quad \text{and} \quad \left(\frac{p}{q}\right)^2 = \frac{\mathbf{m}_{12} - i\Gamma_{12}/2}{\mathbf{m}_{12}^* - i\Gamma_{12}^*/2}. \tag{D8}$$

The time-dependent solution

$$\begin{pmatrix}|M_0(t)\rangle\\ |\bar{M}_0(t)\rangle\end{pmatrix} = \begin{pmatrix}g_+(t) & -(q/p)g_(t)\\ g_+(t) & -(p/q)g_(t)\end{pmatrix}\begin{pmatrix}|M_0(0)\rangle\\ |\bar{M}_0(0)\rangle\end{pmatrix}, \tag{D9}$$

where

$$g_\pm(t) = \frac{1}{2}(e^{-im_H t - \frac{\Gamma_H}{2}t} \pm e^{-im_L t - \frac{\Gamma_L}{2}t}). \tag{D10}$$

For $\mathbf{\Gamma}_{12} \sim \mathbf{m}_{12}$ and $\mathbf{m}_{12}$ is almost real like K^0 system, $\Delta m \approx 2\mathrm{Re}\mathbf{m}_{12}$; while for $\mathbf{\Gamma}_{12} \ll \mathbf{m}_{12}$ like $B_{d(s)}^0$ system, $\Delta m \approx 2|\mathbf{m}_{12}|$. All the measurements and SM predictions are listed here. It is difficult to estimate the long-distance effects that give the dominant contribution in D^0 system.

For decay processes to CP eigenstate f, for example, $B^0 \to \mu^+\mu^-$, the direct observable is the time-integrated averaged branching ratio that has a relation

$$\overline{\mathrm{Br}}(M \to f) \equiv \frac{1}{2}\int_0^\infty (\Gamma(M(t) \to f) + \Gamma(\bar{M}(t) \to f)), \tag{D11}$$

which leads to

$$\overline{\mathrm{Br}}(M \to f) = \frac{1 + A\Delta\Gamma/\Gamma}{1 - (\Delta\Gamma/\Gamma)^2}\mathrm{Br}(M \to f), \tag{D12}$$

where $-1 \le A \le 1$ and in SM $A = 1$.

[1] F. Englert and R. Brout, Phys. Rev. Lett. **13**, 321 (1964); P. W. Higgs, Phys. Rev. Lett. **13**, 508 (1964); G. S. Guralnik, C. R. Hagen, and T. W. B. Kibble, Phys. Rev. Lett. **13**, 585 (1964).

[2] M. Kobayashi and T. Maskawa, Prog. Theor. Phys. **49**, 652 (1973).

[3] N. Cabbibo, Phys. Rev. Lett. **10**, 531 (1963).

[4] CMS Collaboration, Phys. Lett. B **716**, 30 (2012).

[5] ATLAS Collaboration, Phys. Lett. B **716**, 1 (2012).

[6] A. Djouadi, Phys. Rep. **457**, 1 (2008).

[7] The LHC Higgs Cross Section Working Group, Report No. CERN-2013-004.

[8] CMS Collaboration, Report No. CMS-PAS-HIG-14-009.
[9] S. Chatrchyan *et al.* (CMS Collaboration), Phys. Rev. D **89**, 092007 (2014).
[10] P. Govoni (CMS Collaboration), https://indico.ific.uv.es/indico/getFile.py/access?contribId=258&sessionId=23&resId=0&materialId=slides&confId=2025.
[11] CMS Collaboration, J. High Energy Phys. 05 (2014) 104.
[12] ATLAS Collaboration, Phys. Lett. B **726**, 88 (2013); Phys. Rev. D **90**, 095009 (2014).
[13] ATLAS Collaboration, arXiv:1408.5191 [Phys. Rev. D (to be published)].
[14] ATLAS Collaboration, Report No. ATLAS-CONF-2013-030; Report No. ATLAS-CONF-2014-060.
[15] ATLAS Collaboration, Report No. ATLAS-CONF-2013-108; Report No. ATLAS-CONF-2014-061.
[16] CMS Collaboration, Reports No. CMS-PAS-HIG-13-002 and No. CMS-PAS-HIG-13-005.
[17] ATLAS Collaboration, Report No. ATLAS-CONF-2013-013.
[18] The GFitter Group, Eur. Phys. J. C **72**, 2205 (2012).
[19] M. E. Peskin and T. Takeuchi, Phys. Rev. Lett. **65**, 964 (1990); Phys. Rev. D **46**, 381 (1992).
[20] Y. Gao, A. V. Gritsan, Z. Guo, K. Melnikov, M. Schulze, and N. V. Tran, Phys. Rev. D **81**, 075022 (2010).
[21] Q.-H. Cao, C. B. Jackson, W.-Y. Keung, I. Low, and J. Shu, Phys. Rev. D **81**, 015010 (2010).
[22] A. Djouadi, Phys. Rep. **459**, 1 (2008).
[23] M. Perelstein, Prog. Part. Nucl. Phys. **58**, 247 (2007).
[24] A. Farzinnia, H. J. He, and J. Ren, Phys. Lett. B **727**, 141 (2013).
[25] S. H. Zhu, arXiv:1211.2370; Y. Hu, Y. K. Wang, P. F. Yin, and S. H. Zhu, Front. Phys. **8**, 516 (2013).
[26] T. D. Lee, Phys. Rev. D **8**, 1226 (1973).
[27] J. H. Christenson, J. W. Cronin, V. L. Fitch, and R. Turlay, Phys. Rev. Lett. **13**, 138 (1964).
[28] J. Beringer *et al.* (Particle Data Group), Phys. Rev. D **86**, 010001 (2012); K. A. Olive *et al.* (Particle Data Group), Chin. Phys. C **38**, 090001 (2014).
[29] L. Wolfenstein, Phys. Rev. Lett. **51**, 1945 (1983).
[30] C. Jarlskog, Phys. Rev. Lett. **55**, 1039 (1985).
[31] J. E. Kim and G. Garosi, Rev. Mod. Phys. **82**, 557 (2010).
[32] G. 't Hooft, Phys. Rev. Lett. **37**, 8 (1976).
[33] V. Baluni, Phys. Rev. D **19**, 2227 (1979).
[34] C. Baker *et al.*, Phys. Rev. Lett. **97**, 131801 (2006).
[35] A. D. Sakharov, Pis'ma Zh. Eksp. Teor. Fiz. **5**, 32 (1967) [JETP Lett. **5**, 24 (1967)].
[36] Planck Collaboration, Astron. Astrophys. **571**, A16 (2014).
[37] D. E. Morrissey and M. J. Ramsey-Musolf, New J. Phys. **14**, 125003 (2012).
[38] A. G. Cohen, D. B. Kaplan, and A. E. Nelson, Phys. Lett. B **263**, 86 (1991); Annu. Rev. Nucl. Part. Sci. **43**, 27 (1993).
[39] S. L. Chen, N. G. Deshpande, X. G. He, J. Jiang, and L. H. Tsai, Eur. Phys. J. C **53**, 607 (2008).
[40] G. Segrè and H. A. Weldon, Phys. Rev. Lett. **42**, 1191 (1979).
[41] S. M. Barr, Phys. Rev. Lett. **53**, 329 (1984).
[42] S. L. Glashow and S. Weinberg, Phys. Rev. D **15**, 1958 (1977).
[43] T. P. Cheng and M. Sher, Phys. Rev. D **35**, 3484 (1987).
[44] Y. B. Zel'dovich, I. Y. Kobzarev, and L. B. Okun, Zh. Eksp. Teor. Fiz. **67**, 3 (1974) [Sov. Phys. JETP **40**, 1 (1975)].
[45] T. W. B. Kibble, J. Phys. A **9**, 1387 (1976).
[46] L. M. Krauss and S.-J. Rey, Phys. Rev. Lett. **69**, 1308 (1992).
[47] J. Shu and Y. Zhang, Phys. Rev. Lett. **111**, 091801 (2013).
[48] M. F. Parry and A. T. Sornborger, Phys. Rev. D **60**, 103504 (1999).
[49] G. C. Branco, P. M. Ferreira, L. Lavoura, M. N. Rebelo, M. Sher, and J. P. Silva, Phys. Rep. **516**, 1 (2012).
[50] A. Mèndez and A. Pomaral, Phys. Lett. B **272**, 313 (1991).
[51] CMS Collaboration, Report No. CMS-PAS-HIG-13-014.
[52] ATLAS Collaboration, Report No. ATLAS-CONF-2013-052.
[53] R. M. Winters and D. O'Neil, http://people.bridgewater.edu/~doneil/STellipseModule.nb.
[54] W. Grimus, L. Lavoura, O. M. Ogreid, and P. Osland, J. Phys. G **35**, 075001 (2008); Nucl. Phys. **B801**, 81 (2008).
[55] O. Deschamps, S. Monteil, V. Niess, S. Descotes-Genon, S. T'Jampens, and V. Tisserand, Phys. Rev. D **82**, 073012 (2010).
[56] T. Hermann, M. Misiak, and M. Steinhauser, J. High Energy Phys. 11 (2012) 036.
[57] ALEPH, DELPHI, L3, and OPAL Collaborations (the LEP Higgs Working Group) [International Europhysics Conference on High Energy Physics Conference, Report No. LHWG Note/2001-05, arXiv:hep-ex/0107031].
[58] CMS Collaboration, Report No. CMS-PAS-SUS-13-013.
[59] A. D. Martin, W. J. Stirling, R. S. Thorne, and G. Watt, Eur. Phys. J. C **63**, 189 (2009); see also http://mstwpdf.hepforge.org/.
[60] CMS Collaboration, J. High Energy Phys. 02 (2014) 024.
[61] M. Czakon, P. Fiedler, and A. Mitov, Phys. Rev. Lett. **110**, 252004 (2013).
[62] ATLAS Collaboration, J. High Energy Phys. 06 (2014) 008.
[63] CMS Collaboration, Report No. CMS-PAS-HIG-13-034.
[64] ATLAS Collaboration, Eur. Phys. J. C **73**, 2465 (2013); J. High Energy Phys. 03 (2013) 076.
[65] CMS Collaboration, J. High Energy Phys. 07 (2012) 143; Report No. CMS PAS HIG-13-035.
[66] M. Pospelov and A. Ritz, Ann. Phys. (Amsterdam) **318**, 119 (2005).
[67] The ACME Collaboration, Science **343**, 269 (2014).
[68] S. M. Barr and A. Zee, Phys. Rev. Lett. **65**, 21 (1990); **65**, 2920 (1990).
[69] T. Abe, J. Hisano, T. Kitahara, and K. Tobioka, J. High Energy Phys. 01 (2014) 106.
[70] J. Brod, U. Haisch, and J. Zupan, J. High Energy Phys. 11 (2013) 180.
[71] K. Cheung, J. S. Lee, E. Senaha, and P.-Y. Tseng, Report No. CNU-HEP-14-02.
[72] A. Hocker and Z. Ligeti, Annu. Rev. Nucl. Part. Sci. **56**, 501 (2006).
[73] Heavy Flavor Averaging Group, http://www.slac.stanford.edu/xorg/hfag/.
[74] Heavy Flavor Averaging Group, arXiv:1207.1158.
[75] J. Yu, *Proc. Sci.*, LATTICE 2013 (2013) 398.
[76] A. Lenz and U. Nierste, Reports No. TTP11-03 and No. TUM-HEP-792/11.
[77] A. Lenz, U. Nierste, J. Charles, S. Descotes-Genon, A. Jantsch, C. Kaufhold, H. Lacker, S. Monteil, V. Niess, and S. T'Jampens, Phys. Rev. D **83**, 036004 (2011).

[78] J. Laiho, E. Lunghi, and R. S. Van de Water, Phys. Rev. D **81**, 034503 (2010); see also http://www.latticeaverages.org/.
[79] R. S. Gupta and J. D. Wells, Phys. Rev. D **81**, 055012 (2010).
[80] B. McWilliams and O. Shanker, Phys. Rev. D **22**, 2853 (1980).
[81] A. Lenz, U. Nierste, J. Charles, S. Descotes-Genon, H. Lacker, S. Monteil, V. Niess, and S. T'Jampens, Phys. Rev. D **86**, 033008 (2012).
[82] J. Charles, S. Descotes-Genon, Z. Ligeti, S. Monteil, M. Papucci, and K. Trabelsi, Phys. Rev. D **89**, 033016 (2014).
[83] C. Q. Geng and J. N. Ng, Phys. Rev. D **38**, 2857 (1988).
[84] J. Urban, F. Krauss, U. Jentschura, and G. Soft, Nucl. Phys. **B523**, 40 (1998).
[85] E. Golowich, J. A. Hewett, S. Pakvasa, and A. A. Petrov, Phys. Rev. D **76**, 095009 (2007).
[86] LHCb Collaboration, Phys. Rev. Lett. **111**, 101805 (2013).
[87] CMS Collaboration, Phys. Rev. Lett. **111**, 101804 (2013).
[88] CMS and LHCb Collaborations, Reports No. CMS-PAS-BPH-13-007 and No. LHCb-CONF-2013-012.
[89] A. J. Buras, J. Girrbach, D. Guadagnoli, and G. Isidori, Eur. Phys. J. C **72**, 2172 (2012).
[90] C. Bobeth, M. Gorbahn, T. Hermann, M. Misiak, E. Stamou, and M. Steinhauser, Phys. Rev. Lett. **112**, 101801 (2014).
[91] K. De Bruyn, R. Fleischer, R. Knegjens, P. Koppenburg, M. Merk, A. Pellegrino, and N. Tuning, Phys. Rev. Lett. **109**, 041801 (2012).
[92] T. Hermann, M. Misiak, and M. Steinhauser, J. High Energy Phys. 12 (2013) 097.
[93] CMS Collaboration, Report No. CMS-PAS-HIG-13-007.
[94] X.-Q. Li, J. Lu, and A. Pich, arXiv:1404.5865.
[95] M. Misiak *et al.*, Phys. Rev. Lett. **98**, 022002 (2007).
[96] E. Lunghi and J. Matias, J. High Energy Phys. 04 (2007) 058.
[97] CMS Collaboration, arXiv:1307.7135.
[98] H. Okawa (ATLAS and CMS Collaborations), http://moriond.in2p3.fr/QCD/2014/SundayAfternoon/Okawa.pdf.
[99] M. Bicer *et al.* (The TLEP Design Study Working Group), J. High Energy Phys. 01 (2014) 164.
[100] P. Azzi *et al.*, Report No. CMS NOTE 2012/003.
[101] J. E. Brau *et al.* [Open Symposium of the European Strategy Preparatory Group, 2012, Krakow, Poland (to be published)].
[102] W. Liao, http://conf.ccnu.edu.cn/whhep14/docs/highenergy/F2/F2-4/2.LiaoWei.pdf.